THE CATHOLIC UNIVERSITY OF AMERICA

Upper Limb Rehabilitation After Stroke Through Functional Task Focused Intervention

A DISSERTATION

Submitted to the Faculty of the

Department of Biomedical Engineering

School of Engineering

Of The Catholic University of America

In Partial Fulfillment of the Requirements

For the Degree

Doctor of Biomedical Engineering

©

By

Elizabeth Bell Brokaw

Washington, D.C.

2012

Upper Limb Rehabilitation After Stroke Through Functional Task Focused Intervention

Elizabeth Bell Brokaw, PhD

Director: Peter S. Lum, PhD

Stroke results in abnormal muscle synergies, weakness, and spasticity in the affected upper limb, which results in decreased performance of activities of daily living (ADL) and reliance on compensation strategies. Recent clinical reviews have shown the success of functionally motivated clinical intervention, and have shown that recovery of joint coordination is possible and may aid in recovery of real world use of the affected limb. Rehabilitation robots and other devices have become increasingly prevalent for administering arm rehabilitation therapy. The following research shows the benefits of technologies that assist with functional task focused therapy for stroke victims. The research on functional therapy technology was broken into three components.

1) A device, Hand Spring Operated Movement Enhancer (HandSOME), was developed to allow for functional training with real and virtual objects. This device was tested in a cross-sectional study with eight chronic stroke subjects, and significantly improved active range of motion (p<0.001) and functional grasp (p=0.002).

2) A mode of therapy that focuses on normal joint coordination was developed, Time Independent Functional Task Training (TIFT). This mode was validated with thirty-seven neurologically normal subjects and nine stroke subjects. The mode showed improvements

over conventional robotic training modalities in reduction of wall interaction torque, and increased amount of active arm joint coordination during training.

3) Finally, the integrated system of the HandSOME device and TIFT modality with the ARMin III robot was use to training eleven chronic stroke subjects in eight 1.5 hour sessions. After training the subjects significantly improved in Action Research Arm Test score (p=0.01) showing that the therapy improved the subjects' ability to manipulate objects. Overall, the therapeutic system shows potential for improving functional use of the affected arm after stroke.

This dissertation by Elizabeth Bell Brokaw fulfills the dissertation requirement for the doctoral degree in biomedical engineering approved by P. Lum, PhD, as Director, and by S. Ryerson, PT, DSc, A. Roy, PhD, and S. Lee, PhD as Readers.

_____

Peter S. Lum, PhD, Director

_____

Sang Wook Lee, PhD, Reader

_____

Anindo Roy, PhD, Reader

_____

Susan Ryerson, PT, DSc, Reader

ii

DEDICATION

In memory of Eleanore Sauer Brokaw, United States Office of Strategic Services agent during World War II, agent for the United States Central Intelligence Agency, and my loving grandmother. Thank you for being my inspiration to do great things.

TABLE OF CONTENTS

ACKNOWLEDGEMENTS

CHAPTER 1. INTRODUCTION

Each year 610,000 people in the United States have their first stroke (Roger 2012). Although survival rates are steadily increasing, individuals are often left with severe sensory and motor impairment. Even relatively mild impairment of upper-limb function results in considerable limitations in daily function and negatively impacts quality of life (Lai 2002, Nichols-Laron 2005). Among stroke survivors older than 64, fifty percent reported some hemiparesis at six months post stroke and twenty-six percent reported being dependent in activities of daily living (Roger 2012). This results in increased expense for caregivers, and increased incidents of depression, in stroke survivors. New therapeutic strategies will hopefully improve stroke survivors' quality of life.

1. STROKE CHARACTERISTICS

Stroke occurs when blood flow is lost to an area of the brain resulting in tissue damage. Although this can occur in many different areas of the brain, resulting in a wide variety of symptoms, stroke often affects movement control of the side of the body contralateral to the injury site. In the acute phase, less than 6 months post stroke, this often presents as paralysis on the affected side of the body. In the chronic phase, stoke typically presents as weakness, the loss of inter-joint coordination, abnormal muscle synergies, and hypertonia in the affected side of the body. These symptoms severely impair function for stroke survivors during activities of daily life such as reaching and grasping movements. Studies have reported a variety of impairments during reach to gasp tasks, including decreased

muscle activation and weakness (Bohannon 1991), disrupted inter-joint coordination (Dipietro 2007), decreased smoothness of movement (Rohrer 2002), and dyscoordination between reach and grasp movements (van Vliet 2007)

Abnormal Muscle Synergies

Muscle synergies are the coupling of muscle bodies during activation. Abnormal muscle synergies restrict movements where the coupled muscles are normally fired independently. Abnormal muscle synergies after stroke are often characterized into the "extensor" and "flexor" synergies. The flexor synergy is the simultaneous firing of elbow flexion with shoulder abduction and or shoulder elevation. The extensor synergy is less common but is characterized by elbow extension with shoulder adduction. These abnormal synergies result in the loss of normal joint coordination that is hypothesized to be essential for functional recovery (Lum 2002). While this impairment can be overcome with compensatory strategies (excessive trunk movement), recovery of inter-joint coordination is possible with a focused intervention (Ellis 2005). Importantly, therapy strategies that promote relearning of normal inter-joint coordination and movement kinematics may have critical effects on actual real-world use of the limb in ADLs (Lum 2009), while therapies that allow use of compensatory strategies may actually impede this process (Krakauer 2006, Roby-Brami 2003).

Figure 1.1. Image of a chronic stroke subject reaching to a target placed beyond full arms length. The elbow flexion resulting from shoulder elevation can be seen looking from the left to the right image.

Muscle Weakness

Weakness after stroke is frequently due to the disrupted neurological control pathways and nonuse of the limb resulting in muscle loss. In the acute phase, weakness is the predominant symptom due to hemiparesis. Weakness is also a key factor in chronic stroke impairment. The loss of muscle mass due to nonuse can results in the loss of normal muscle tone. For example, stroke patients may lose the normal muscle strength holding their shoulder joint resulting in the partial dislocation, also known as subluxation, of the shoulder. The resulting abnormal postures during movement may result in joint injury during training.

Spasticity and Hypertonia

Spasticity is defined as the velocity dependent resistance to passive stretch (Lance 1980). This often leads to difficulty with precise movement control. Hypertonia is similar to

spasticity and the terms are often used interchangeably. However, for the purposes of this paper, we measured hypertonia as the slow passive movement stiffness, sometimes called 'soft tissue tightness', as was measured by Kamper et al. (Kamper 2003). Hypertonia is commonly observed in the elbow, wrist, and finger flexors after stroke, resulting in the pathology shown in the image below.

Figure 1.2. Subject assisting his at his wrist to move his hand over the block and keep his wrist in the neutral position. However, due to hypertonia and extensor weakness, he cannot extend his fingers enough to grab the block.

The Stroke Hand

The impairment of the hand after stroke is often considered to be the main factor limiting functional use of the arm. At three months post stroke 38% of patients reported major difficulty with hand function (Duncan 2003). In the chronic stages of stroke the finger flexors become hyperactive, especially across the proximal and distal phalanxes. This often causes a patient's command to open their hand to result in closing of the fingers. At the same time normal tone that preserves the palmer arch and maintains normal grasp

postures can be lost. Independent finger movement as well as inter-joint coordination of the fingers and thumb is often also lost, resulting in difficulty with coordinating the hand into proper grasping postures. Figure 1.3 shows the common impairment of the chronic stroke hand.

Figure 1.3 Subject in the HandSOME device cross sectional study described in chapter 2. The image shows the tightness of the finger flexors and the loss of joint control, which has prevented normal opposition by the thumb during grasp.

Movement Symptoms

Arm movements after stroke are characterized by a loss of active range of motion and movement smoothness. Independent joint control of the arm is also typically lost after stroke. This loss of normal coordination is combined with the effects of muscle weakness, abnormal synergies, and hypertonia of other muscle groups. This causes difficultly in many fine motor skills and movements that require coordinated joint movement.

Clinically these upper extremity impairments are measured through tests such as the Action Research Arm Test (ARAT) (Yozbatiran 2008), upper limb section of the Fugl-Meyer (Fugl-Meyer 1975), Box and Blocks (Desrosiers 1994), and the Modified Ashworth Scale (Gregson 1999). The ARAT examines a patient's ability to grasp and manipulate objects. The upper limb section of the Fugl-Meyer looks at reflexes of the arm and how the arm movement is affected by abnormal synergies. The Box and Blocks test measures how many blocks a subject can move across a barrier in one minute. This test gives a quick measure of functional hand use. The Ashworth is a 5-point rating scale for measuring muscle tone, with ratings of 0 for no increase in tone up to a score of 4 for a rigid limb. The therapist examines the joint, such as the elbow, by bringing the flexed joint to maximal extension in one second. The therapist then gives a score based on the resistance to movement and any sudden resistive catch that is felt. Although patient and rater variability both limit the use of these tests, the measures allow researchers and clinicians to examine the potential therapeutic methods that will benefit the patients the most.

2. CURRENT STROKE THERAPY METHODS

Current therapeutic methods for the arm after stroke have been focused on regaining passive range of motion, then full active range of motion and strength training (Donaldson 2008). However, the ability for strength training to improve functional use of the limb has not been shown and recent articles suggest that functional goals should play a larger role in therapy (Timmermans 2009). Stroke rehabilitation is now shifting its focus to include more functional task training after reviews have shown that impairment

focused therapies have less successful impact on the recovery of ADL than functional task training (Van Peppen 2004). Therapists often train compensation movement patterns to assist with completion of activities of daily living. However, studies have shown that recovery of joint coordination is possible (Ellis 2005) and may aid in recovery of real world use of the affected limb (Lum 2009). Repetitive use of the affected arm has been shown to be an effective method for improving motor function (Taub 2002). Novel technologies, such as therapeutic robotic devices allow for increased repetitions.

3. CURRENT TECHNOLOGIES

Robotic therapy systems allow for very precise and reproducible therapeutic regiments. This allows for easier comparison between therapeutic methods as compared to conventional therapy and for direct and numerical ability comparisons between days of training. Robots can also provide tailored assistance in tasks to elicit maximal patient exertion, while still allowing the patient to complete the tasks and avoid frustration. There are many training technologies for stroke rehabilitation. These devices range in complexity from single joint passive (no motor) devices to full arm exoskeletons with 6 active degrees of freedom (DOF).

Passive Arm Rehabilitation Devices

Passive devices are able to provide motor assistance during therapy with less weight, and lower cost than active systems. Several passive arm rehabilitation devices have been developed to aid with stroke recovery. These devices provide arm weight compensation using overhead pulley systems (Stienen 2007, Prange 2009, Riener 2005), spring-based

arm orthotics attached to wheelchairs (Herder 2006, Rahman 2007) and passive exoskeleton rehabilitation devices (Housman 2009, Stienen 2007). The Saeboflex® is an example of a passive hand rehabilitation device that has been successful in assisting with opening the grasp of stroke patients and is commonly used for tone management therapy (Farrell 2007). However, this device is not intended for functional grasp of diverse objects, as it was designed only for picking up objects 3-4" in diameter and smaller objects cannot be grasped. The springs that are connected to the distal phalanx of each finger provide increasing force with increasing finger flexion, which makes it difficult to obtain and maintain full flexion even with low force springs, limiting range of motion. Another passive hand device used for motor training is a cable driven orthotic by Fischer et al. (Fischer 2007). However, this device requires the subject to use shoulder and elbow movement to assist with finger extension, which decreases the ability for normal movement kinematics in reach and grasp task training.

Rehabilitation Robotics

Active devices allow for more dynamic assistance and movement guidance than passive devices. The complexity of active systems in the field of rehabilitation robots varies greatly. Single degree of freedom robots, for example elbow or wrist robots, focus therapy on a single affected joint of the arm. Although it is likely that this treatment will be beneficial for regaining passive and active range of motion in a single joint, it is unlikely that it will have a large effect on overall functional impairment of the arm since the simplified system can not allow for the practice of functional activities.

More complex systems allow for movements of multiple degrees of freedom of the arm. Studies with the first robots, MIME (Lum 2002), ARM Guide (Kahm 2006), and the MIT Manus (Aisen 1997), showed that the devices could provide safe assisted movements during training that resulted in motor improvements. These robots are end point devices that focus on the position of the hand during planer reaching. A recent multisite study with MIT Manus showed therapy with the robot was comparable to dose-matched conventional therapy but superior in motor function scales at the 36-week follow up (Lo 2010). Meta analysis and systematic reviews of clinical trials have shown that use of upper limb robots have some advantages in recovery of strength and movement ability when compared to active control groups that did not use robots; but there were no advantages in recovery of ADL ability (Prange 2006). Exoskeleton robots, such as the ARMin III rehabilitation robot (Nef 2007) used in this study, allow for control of six degrees of freedom in independent as well as coordinated joint training. This allows for the most realistic functional robotic training, which will hopefully improve function in ADL. In order to do this, a hand component must be created to help train functional activities. The hand component is often ignored in these arm robots. In some cases a force sensor may be used on the end point dowel, but this still provides very limited functional training.

The majority of hand devices currently on the market are active systems powered by electric or pneumatic motors. This leads to an increased device weight due to the inherently large weight of motors and power supplies relative to the weight of the human hand. As a result many of these devices could not be held at the end point by the current

motors on the rehabilitation robots or by patients with proximal arm weakness. Many of these devices also utilize internal grasp structures (Bouzit 2002, Masia 2007, Lambercy 2007), which diminishes the possibility of use with real world objects, and can limit range of motion (ROM). Current actively powered external grasp devices are also exceedingly bulky and limit the type of grasp and hand orientation that can be used for task practice (Balasubramanian 2010).

Robotic Therapy Software

Although some potential benefits of robotic therapy are known, the way that the robot should interact with the patient is still debatable. The basic levels of control range from passive therapy, active assist/time dependent mode (subject is told to move with the device), active, and resistive. Rehabilitation modes are moving away from passive and active assist modalities, except in extremely low function patients, due to concerns about decreased patient activity during training leading to decreased improvements (Hidler 2009). The main area of research development is the patient active training. This still leaves a wide possibility for control strategies. One common method uses end point tunnels to help guide the patient's hand along the path. However, this has several limitations: 1) in multiple joint robots abnormal compensation patterns will be used, such as internal rotation of the shoulder 2) guiding walls may be used to achieve the task without correct active movement.

4. THE GOALS OF THE FOLLOWING RESEARCH

The limitations in stroke hand devices and robotic therapy modes have been addressed in this work. The following research presents some novel technologies for upper limb rehabilitation after stroke. <u>The overall goal of this research was to develop a system for stroke rehabilitation that focuses on interactive functional training with normal movement coordination</u>. This research is divided into three sections:

1. Section 1 covers the development and testing of a hand device, Hand Spring Operated Movement Enhancer (HandSOME), which assists with interjoint coordination of the hand and finger extension after stroke for functional training with the ARMin III robot. HandSOME provides a large finger range of motion and allows grasp of both small and large real world objects in even severely impaired subjects. This device has a lightweight design to minimize the impact of patient shoulder weakness and ARMin III motor strength limitations. The HandSOME device uses a 4-bar linkage to assist patients with lost independent joint coordination after stroke, and allows for real and virtual object manipulation. The possibility for independent home use of the HandSOME device was also explored.

2. Section 2 covers the development and testing of a novel robotic training mode, Time Independent Functional Task Training (TIFT), for the ARMin III exoskeleton robot. This mode requires stroke subjects to actively use normal joint coordination to complete functional tasks. For example, in the shelf task the stroke subject must learn to overcome the abnormal flexor muscle synergy to elevate their shoulder while they extend their

elbow at the same time. It was hypothesized that when compared with other training modes, TIFT would provide faster reduction of error due to its focus on active subject joint coordination during movement training. This mode was validated in motor learning study comparing the TIFT mode to active assist (time dependent) mode and visual feedback in neurologically normal subjects.

3. In the final phase of the study the new modality and the HandSOME device were combined for functional training of chronic stroke subjects. The combination of the new mode and hand device allow for real and virtual object manipulation during properly coordinated tasks. The robot allows for large numbers of task repetitions, variable task difficulty, and can provide assistance through arm weight compensation as needed.

CHAPTER 2. HAND SPRING OPERATED MOVEMENT ENHANCER

In stroke survivors, hand function is often impaired by the loss of normal interjoint coordination, flexor hypertonia (increased resistance to passive finger extension) and weakness in finger extensors. Unfortunately, fine function of the fingers is necessary to perform many activities of daily living (ADL) and thus stroke patients are often very dependent on compensatory strategies. The goal of this research was to develop a lightweight, passive, wearable device that assists with hand function during performance of activities of daily living (ADLs) and can be incorporated into a therapy program with the ARMin III robot. The device was also examined for the possibility of independent home-based training protocol for stroke survivors.   Details about the design development can be found in my master's thesis (Brokaw 2009) and some of the following information and figures were originally published in IEEE Transactions on Neural Systems and Rehabilitation Engineering (Brokaw 2011).

The Hand Spring Operated Movement Enabler (HandSOME) is a passive, lightweight hand rehabilitation device that overcomes many of the limitations of current rehabilitation devices. HandSOME provides a large finger range of motion and allows grasp of both small and large real world objects in even severely impaired subjects. The HandSOME device was designed based on the biomechanics of the hand after stroke. Kamper et al. found a nearly linear relationship between metacarpalphalangeal (MCP) joint extension angle and applied extension torque in the hypertonic finger joints of stroke subjects (Kamper 2003, Kamper 2000). They also found that stretching of the

flexors was correlated with muscle activity in the paretic extensors. HandSOME provides increasing extension assistance with increasing finger extension angle. The majority of stroke subjects have the ability to flex their fingers voluntarily, so assistance for flexion is generally not required.

HandSOME was designed to assist the hand with coordination and grasp release for the pinch-pad grasp, which brings the pads of the thumb and fingers together and contrasts with a power grasp where the thumb wraps around the fingers. Pinch-pad grasp can be used to grab object of many different shapes and sizes and is commonly used in activities of daily living (ADL). The simplification to training a single gross grasp posture was motivated by the fact that stroke survivors often must rely on gross grasp for ADL due to loss of independent finger movement, finger proprioception, and fine touch sensation (Raghavan 2006). Although different therapy methods may be needed to help retrain more dexterous movements, restoration of hand use in ADL through gross grasp and release training will likely improve many stroke survivors' quality of life. The HandSOME device uses a linkage between the finger and thumb actuating components to ensure proper inter-joint coordination during grasp. This design will allow stroke survivors with lost independent joint control to obtain and hopefully retrain proper inter-joint coordination in grasp (Raghavan 2006, Lang 2004)

The HandSOME device utilizes increasing assistive torque with increasing extension angle with passive actuation via elastic cords to assist with finger and thumb extension. Passive actuation, as well as the use of light-weight materials, allows for a wearable

design, which increases portability. The HandSOME device was tested for comfort, the effect on ability to perform simple ADL, the effect on active range-of-motion (ROM), and the potential negative effect on grip strength in individuals with various levels of flexor hypertonia due to stroke.

1. HANDSOME DESIGN

The angle of grasp is measured using a small encoder (E4 Series, US Digital, Resolution 0.25 degrees) or a potentiometer. A 4-bar linkage was designed to force normal thumb and finger coordination in the pinch-pad grasp. The HandSOME design uses elastic cords as spring actuators to assist with finger and thumb extension, and provide assistance profiles that emulate the torque vs. extension angle profiles for passive movement reported by Kamper et al (Kamper 2003). Changes in the spring location and stiffness used allow the therapist to vary the assistance profile and magnitude.

Although two design versions were used in stroke subject testing, the two designs were identical in terms of the critical features of the HandSOME device. The finger-thumb linkage and the assistance torque profiles remained unchanged between versions. Version 2 decreased the weight and general profile of the device. This difference between versions 1 and 2 of the device did not affect performance of the study tasks because subjects were allowed to support the paretic arm with their other arm if needed. Therefore, test data from all subjects were grouped together for analysis. All images shown in this paper depict the second version of the device. Figure 2.1 shows the latest completed design and the hand interface.
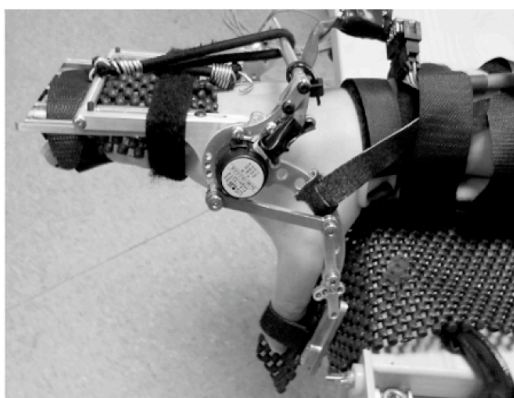
Figure 2.1 The image shows the HandSOME device fitted to a stroke subject with hypertonia

The tested devices weigh 0.22 kg (version 1) and 0.128 kg (version 2). The device is able to accommodate a maximum finger length of 0.13 m and a maximum hand width of 0.1 m, with no minimum hand width or length. These hand measurements represent the 99th percentile for male hands (Chengalur 2004).

Adjustable mechanical hard stops are used to control the range of motion. This prevents over extension to subjects who cannot tolerate full range of motion. Padding and supporting straps were added to the device for comfort and to maintain ideal positioning of the device on the back of the hand throughout the movement. The Velcro straps were positioned distally to prevent the fingers from curling around the straps. One strap was placed across the hand at the distal phalanx of the pinky and another at the proximal interphalangeal joint (PIP) of the pointer finger. If needed, a third strap was used across the distal phalanges of the middle three digits. A single Velcro strap was used at the interphalangeal joint (IP) of the thumb. Therefore, the straps restricted movement of the

thumb IP, finger DIP and finger PIP joints. The main movement for the pinch pad grasp is rotation at the MCP of the fingers and the carpometacarpal joint (CMC) of the thumb. A wrist brace was used for subject testing to maintain neutral wrist posture in the device and to ensure proper orientation of the HandSOME device on the subject's hand. Various adjustments can be made to adapt for different size hands. The finger and thumb attachment points can be extended to match finger length and the thumb attachment component can be rotated to match the subject's thumb orientation.

<u>Linkage Design</u>

The HandSOME device was designed to smoothly follow the movement of the human hand for comfort and proper retraining of normal grasp movement by modeling the kinematics of the hand during the pad-pinch grasp. The hand movement was measured using an acoustic based three-dimensional motion tracking system (Zebris CMS-HLS). The markers were placed on the distal ends of the pointer finger and thumb as well as at the metacarpal phalangeal (MCP) joints. Five repetitions of the pinch-pad grasp were recorded and the angles of rotation and coordination of the fingers and thumb were calculated. The finger MCP and thumb carpal metacarpal (CMC) joint positions were used as the rotation centers of the device. Analysis of the kinematics of several normal subjects showed synchronous movement coordination between the fingers and thumb with a range of motion of approximately 78° in the fingers and 39° at the thumb. To accommodate full passive ROM, the design specification for the linkage was defined as synchronous movement of 90° at the finger MCP and 45° at the thumb CMC.
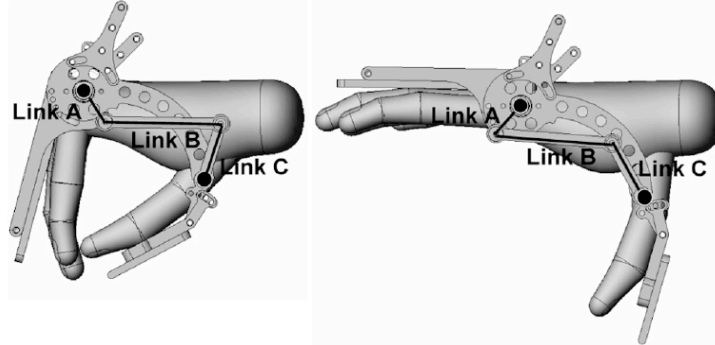
Figure 2.2 The 4-bar linkage of HandSOME. The dark circles designate the ground points of the linkage (finger MCP and thumb CMC). The line between these two points (not shown) designates link G of the 4-bar linkage. The black lines are the links A, B and C.

A 4-bar linkage was designed to maintain the relative angles of the fingers and thumb during the modeled grasp (Fig. 2.2). The ground locations were placed at the finger MCP and thumb CMC since these are the approximate centers of rotation of the hand during the pinch-pad grasp. Although there are many possible linkage solutions that maintain the desired relative angles, linkage options were reduced based on their ability to avoid singularities, minimize link forces, minimize link lengths, and to not impeding grasp or view of the palm of the hand. The resulting 4-bar linkage is shown on the HandSOME device in Fig. 2.2. The actual ROM of the tested device was 90° at the finger MCP and 52° at the thumb CMC.

Torque Profile By Spring Location

The ability to control finger extension assistive torque profile is important for customizing device assistance to the patient's disability. The HandSOME design goals were: 1. a potential torque magnitude greater than 4 Nm in the fully extended position, 2. decreasing extension torque as the fingers flex to a closed position to minimize fatigue, and 3. minimal spring length change over the ROM due to spring in bungee cord material limitations.

Four Nm was chosen based on pilot testing measurements of finger extension torques with high tone patients; however higher peak torque values can be achieved simply by increasing spring stiffness by placing more elastic cords in parallel. The requirements for the linkage, spring properties, and the kinematics were input into a static model of the device to analyze a 2-dimensional grid of possible locations for the spring ground and distal attachment locations. Examination of solutions determined that the most linear assistance profiles resulted from a spring path that goes through the center of rotation of the finger MCP when the hand is closed, thus completely eliminating the applied torque in this posture. To allow adjustment of the assistance profile for different patients, a series of ground point locations was selected that varied the amount of torque applied in the fully closed position so patients with extreme extensor weakness cans still use the device. The system was then tuned for spring constant, spring rest length, and distal spring attachment point. This tuning involved examination of the torque assistance profiles with each possible design, with the goal of selecting spring characteristics that yielded an approximately linear torque assistance profile.

The final design is shown is Figure 2.3. The ground point of the spring is located at the end of a level arm that can be rotated to change the assistance profile. When the lever arm is in its normal position, the spring path goes through the center of rotation of the finger MCP when the hand is in full finger flexion (0 degrees of finger extension). Theta is defined as the angle of the lever arm relative to this normal position. By rotating the lever arm away from this normal position, the therapist is able to change the shape of the assistance profile and increase the amount of assistance applied in the fully closed position. This allows individuals with no extension ability to use the device by simply relaxing their hand, causing the device to open their hand for them, whereas the Theta=0 setting will require some ability to extend volitionally from the fully closed position. The different torque profiles theoretically available are also shown in Fig. 2.3.
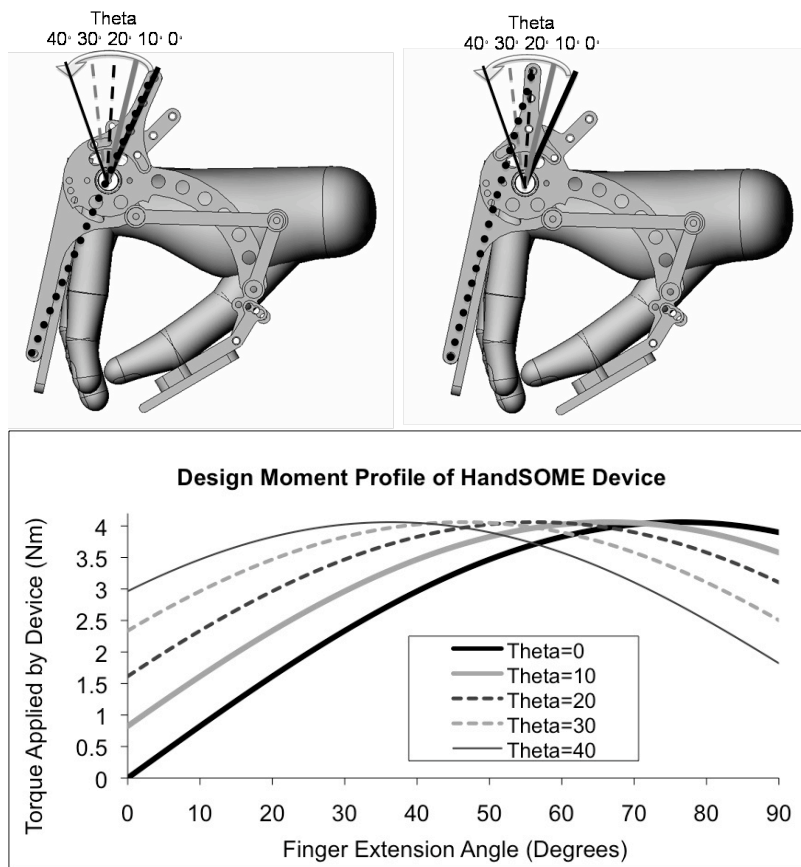
Figure 2.3. The top images show the possible Theta settings for the HandSOME device, which determines the spring line of action. The images show the device at 0 degrees of finger extension. At Theta=0 (top left image) the elastic cord line of action, as shown with the black dotted line, is directly through the center of rotation of the MCP when the device is in the fully flexed position and no assistance torque is applied. The other Theta settings are defined as an angle relative to the Theta=0 line of action. The elastic cord line of action for Theta=20 is shown in the top right image. The bottom plot shows the torque profiles corresponding with the different Theta settings.

These diverse profiles can be used to match the tone profile of the subject, which will maximize the subject's range of motion and grip strength in the device. The actual torque profile was measured by attaching a force/torque sensor (JR3 Inc., Model: 67M25A) to the device and measuring the torque required to slowly open and close the device (no hand in device). The measured profiles were very similar to the theoretical calculations. We calculated the error between theoretical and experimentally measured torque profiles and found that with 5 springs attached, the average error across the full ROM of the device was 0.007 Nm for Theta=0 deg, and 0.036 Nm for Theta=10 deg. Using the same method without any springs attached, friction of the device was measured and found to be mostly constant through the device ROM with a maximum value of 0.038 Nm.

Elastic Cord Choice

The choices of spring attachment points were affected by the maximum extension ratios (the max spring length divided by the initial length) and spring constant (k) values of the potential actuators. Elastic cords were chosen instead of metal springs due to their higher extension ratios. Even with elastic cords, their limited extension ratios caused the peak of the torque profile to be moved to a more flexed position than the desired fully extended angle. The chosen elastic cords (Joubert 10" Mini Bungee, k=74.6 N/m) are easily attached to HandSOME and stiffness can be increased by simply adding more cords in parallel.

2. HANDSOME USE TESTING

The goal of this testing was to examine comfort, patient acceptance, and functional use of the device in subjects with severe to moderate hand impairment. Tests examined the ability of the device to increase ROM, improve performance in functional activities as measured by a block lifting task, and the effect of the device on the subject's grip strength. Inclusion criteria were a clinical diagnosis of stroke, elevated tone in the fingers, and absence of pain in the hand/wrist area. Eight stroke subjects were tested and their general information is shown in Table I. The clinical measurements were done before device testing by a trained occupational therapist. Upper extremity movement impairments at the shoulder, elbow, wrist and fingers were evaluated with the Fugl-Meyer Assessment (Fugl-Meyer, 1975). It scores reflexes and the ability to perform several simple movements and tasks on a 3-point scale. A maximum summed score of 66 indicates no impairment. Muscle tone was measured in the finger flexors with the Modified Ashworth Scale (Gregson 1999). The Ashworth is a 5-point rating scale for measuring muscle tone, with ratings of 0 for no increase in tone up to a score of 4 for a rigid limb. All testing was approved by the MedStar Health Human Subjects Institutional Review Board.

TABLE I. SUMMARY OF SUBJECT CHARACTERISTICS

Subject #	1	2	3	4	5	6	7	8
Gender	F	M	F	M	F	F	M	M
Affected Hand	L	L	L	L	R	R	R	L
Time Post Stroke (yrs)	6	2	1	1	3.5	5.5	0.4	0.17
Ashworth, Finger Flexion (0-4)	1+	1+	1+	2	1+	2	1+	2
Fugl-Myer Upper Extremity (0-66)	28	15	5	19	43	37	16	24

F=Female M=Male L=Left R=Right

Biomechanical Tone Examination

Characterization of hypertonia can be difficult due to the highly variable nature of the hyperactivity of the finger flexors. In order to get a general idea of the magnitude and profile of the subject's tone, the following experiment was performed before device testing. A force-torque sensor (JR3 Inc., Model: 67M25A) was attached to HandSOME at a known distance from the finger component's center of rotation. The subjects were fitted into the device without springs attached and told to relax their hand while the researcher moved the subject's hand through their comfortable ROM three times at approximately 5° per second. The friction and gravity torques from the device during movement were subtracted from the measured torque profile.

<u>Selecting Ideal Spring Settings and Range of Motion Testing</u>

The following procedure was used to determine the ideal spring settings for each subject. To determine the best match to the subject's tone profile, three different torque profile settings were tested for each subject: Theta = 0°, 20°, and 40° for the first version of the device and Theta = 0°, 10°, and 20° for the second version of the device. The Theta= 30° and 40° settings were eliminated in the second version of the device since initial subject trials indicated there was no need for these extreme settings. The patient was asked to extend and flex their hand in the device three times at their own pace to obtain the unassisted free ROM. The subject was then asked to relax their hand and springs were then added until the patient's hand was in full extension. Again, the patient was then asked to close and open his or her hand three times. These angles were recorded to determine the subject's maximum range of motion and movement profiles. The same fitting and testing procedure was used with each Theta setting. The Theta setting with the smallest number of springs and largest consistent range of motion was used in the functional testing as the ideal HandSOME setting for that subject. Paired t-tests were performed on range of motion and peak movement velocity with and without spring assistance from HandSOME.

<u>Functional Testing</u>

The HandSOME device's capacity to increase performance of functional activities was measured in a task modeled after the Box-and-Blocks task (Marteniuk 1990). Subjects were asked to move his or her hand from a start position to a block, lift the block off the table about 3" and then put it down again. Since lifting the object was meant to show that

the subject had a firm grasp on the block and we did not want proximal arm weakness to affect the data, the subject was allowed to use their unaffected limb to assist with the lifting and transport process by supporting the paretic forearm if needed. The blocks used were all of equal height and length but varied in width from 1/2" to 4". The functional testing was performed with and without the device. Subjects were allowed to rest and stretch their hand as needed during testing outside of HandSOME, but stretching was not allowed during testing inside of HandSOME. The time required to complete each task was recorded with a stopwatch to get a general measure of ease of movement. Stopping to stretch the hand was considered the end of an attempt and not included in the time recording. Subjects were informed that they did not need to rush, the pacing of movement was their choice, and that the time was only being recorded to compare between the hand alone and HandSOME trials. Functional testing of the hand alone was performed first to avoid potential increased hypertonia from repeated effort over the course of the test session. This functional testing was performed after the ROM testing, which determined the ideal HandSOME setting. Paired t-tests were performed on the largest block that could be lifted with and without HandSOME.

Grip Strength Testing

One potential concern with the HandSOME device design is that the subject's grasp force may be decreased by the springs. This was tested by asking the subject to grasp a force sensor as strongly as possible for two seconds and then relax for three seconds (grip aperture=0.04m). Since the subject's hand is not completely closed, the springs are providing an extension torque to the fingers as they squeeze the sensor. This procedure

was repeated three times with the subjects in the HandSOME device, first without spring assistance, and then again at their ideal spring settings. Paired t-tests were performed on peak grip force with and without HandSOME.

3. HANDSOME USE TESTING RESULTS AND DISCUSSION

Eight stroke subjects with a relatively wide range of functional ability were tested. The subject feedback on the HandSOME device was positive. Subjects commented that the device was generally comfortable and did not have any pressure points. Most of the subjects reported that they would be interested in using the device at home. The first four subjects were tested with version 1 of the HandSOME device (Brokaw 2010). Some of these subjects reported some difficulty in arm transport due to shoulder weakness and the device's weight. This problem was addressed in version 2 of the device and no subjects using this version reported added difficulty with arm transport. The major difference between the two versions of the device is weight, which should not have a significant effect on testing since subjects were allowed to use their unaffected arm to assist with transport of the objects in functional testing. Therefore data from both devices were collapsed for group analysis.

Maximum measured hypertonia varied between 0.2 and 0.8 Nm across subjects. The mean tone profile for all the subjects linearly increased with finger extension angle with an R-square value of 0.95. The resting hand posture was often not the fully flexed position (defined as 0 degrees of extension), so many of the tone profiles begin at around 20 degrees of extension. The subjects generally showed the linear increase in torque

with extension angle as described in previous studies (Kamper 2003, Kamper 2000). Figure 4 shows the tone of two subjects who used an ideal spring setting of 3 springs. The figure shows that while one subject had a good match between tone and assistance torque at full extension, the other subject did not, possibly due to changes in tone over the course of the test session. In half of the subjects, the tone and assistance levels matched at full extension, which was the goal of the fitting procedure.
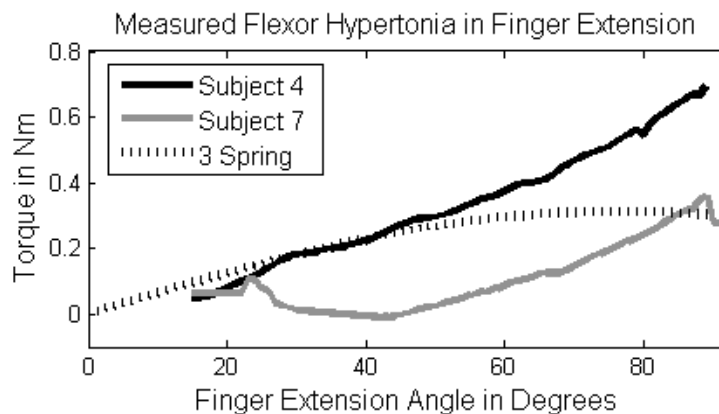
Figure 2.4. Tone data of two subjects who used the 3 spring setting. Some subjects showed good matching of tone and assistance torque at maximum extension, while other subjects did not.

Theta=0° was the ideal setting for 7 out of 8 subjects since they were able to move out of the fully flexed position, and had the lowest required spring force at this setting.   The optimal setting for subject 7 was the Theta=10° position. Although this subject had a slight amount of volitional extension, in ROM testing his movement was not consistent and he would occasionally get stuck in the full flexion position with the Theta=0° setting. The Theta=10° setting allowed consistent volitional extension away from the fully flexed

position. Across all subjects, the optimal spring stiffness settings ranged from 2 to 5 springs. For 2 springs and Theta=0, the applied torque was 0 Nm with the hand closed and increased up to 0.2 Nm with the hand fully extended. For 5 springs and Theta=0, the extension torque at full extension was 0.5 Nm.

The range of motion increased with use of HandSOME (p<0.001). All subjects had increased maximum ROM (max extension angle - min extension angle) with the HandSOME device, with an average increase of 48.7±1.0 degrees of extension with the ideal HandSOME device settings as compared to the unassisted hand free condition (Fig. 2.5).
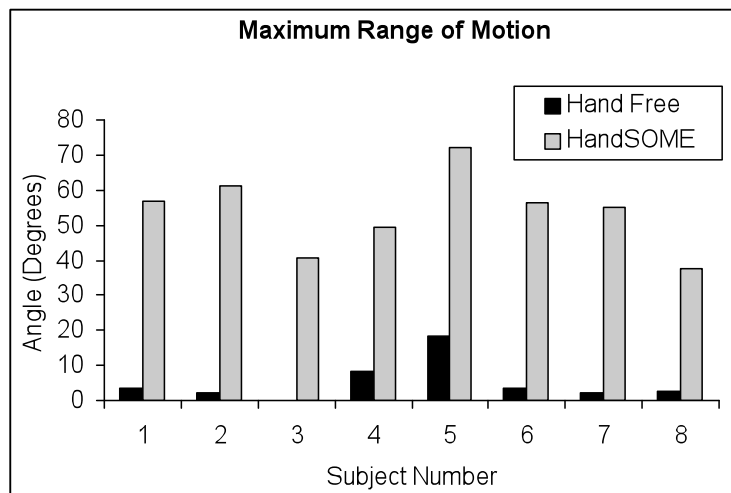

Figure 2.5. Maximum range of motion (max extension angle - min extension angle) of the fingers with and without spring assistance from the HandSOME device. No range of motion is shown for subject 3 in the hand free condition since the subject could not produce any finger extension.

Subjects produced smooth movements in the device both in flexion and extension although the time for the extension movement was much larger than for flexion. In flexion, subjects showed a significant (p=0.004) peak velocity increase from 26.9±13.9 (mean±standard error of the mean, SEM) degrees per second with the unassisted hand to 93.1±24.76 degrees per second with the HandSOME device. Velocity in extension also increased from 11.3±4.45 degrees per second with the unassisted hand to 59.4±22.34 degrees per second with the HandSOME device, and this difference approached significance (p=0.053). Figure 6 shows the range of motion data of a single subject. Performance of this subject when assisted by HandSOME was very typical across subjects.
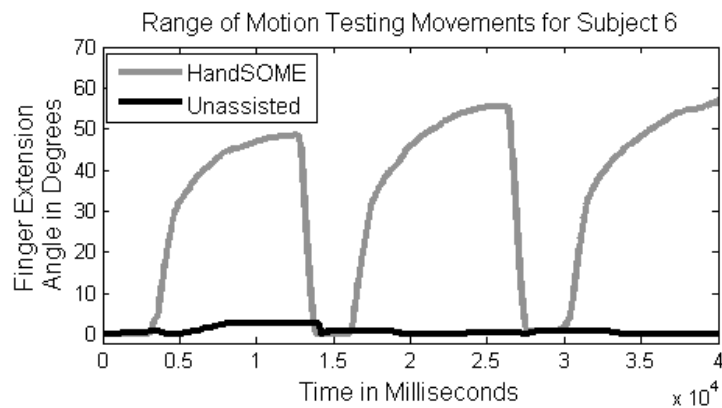

Figure 2.6. Subject 6's movements in the HandSOME device with and without assistance from the HandSOME device. The other subjects had similar profiles, although the unassisted movements were sometimes much less consistent, with the three attempts resulting in only a single movement.

The goal of the block lifting task was to determine if using HandSOME increased the size of the largest object that could be lifted while not impairing the ability to lift smaller objects that subjects could already lift unassisted. Group analysis found that using the HandSOME device increased the size of the largest block that could be lifted (p=0.002). All subjects had improvements in the functional block testing with the HandSOME device. Figure 2.7 displays movement times and the largest successfully lifted block width for each subject with and without the HandSOME device.

In all cases, subjects were successful in lifting all blocks that were smaller than the largest lifted block. For example, subject 1 could not lift any of the blocks unassisted, but lifted all blocks from ½" up to the 3" with HandSOME. There was little difference between hand free and HandSOME testing in terms of the average time for a successful lift in subjects 5, 6 and 8. The time data for subject 3 was lost. However, subjects 4 and 7 had the largest movement times in the hand free condition and had dramatic reductions in movement time when assisted by HandSOME. Subject 4's movement time improved from 25.6 seconds to 7.3 seconds with HandSOME, while subject 7's movement time went from an average time of 41.1 seconds to 8.6 seconds per block. Since the subjects were told to move at their own pace, the large change in movement time showed that in these two subjects, the tasks were generally easier with the HandSOME device.
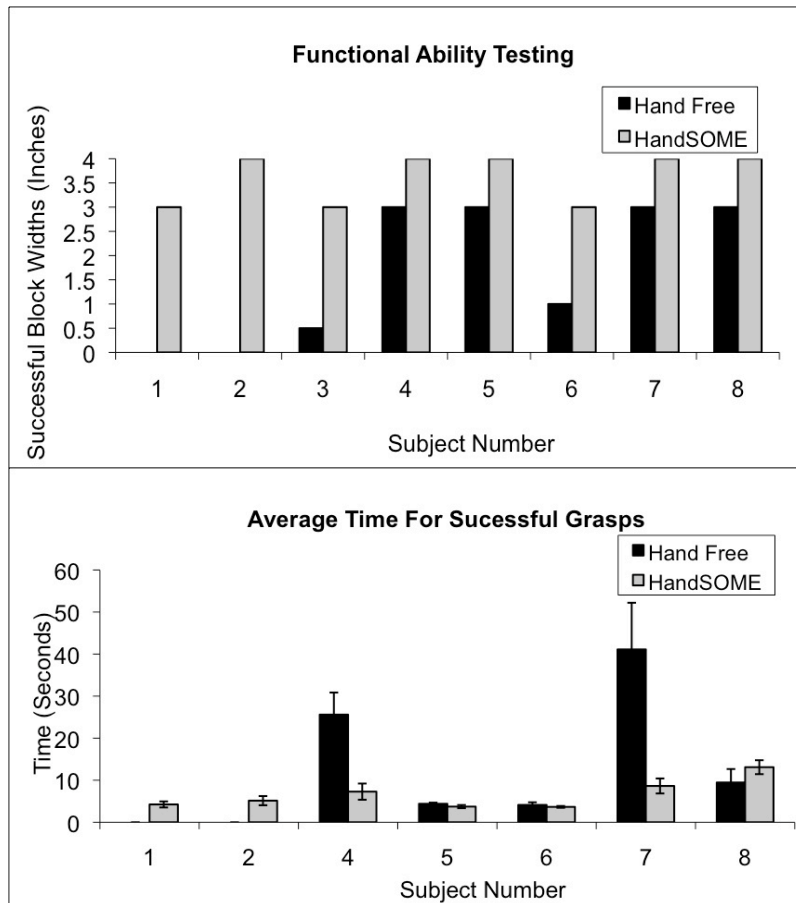
Figure 2.7. The top panel shows the largest successfully lifted block width with and without HandSOME. All smaller blocks were successfully lifted in each case. The panel on the bottom shows the average self-paced time for a successfully lifted block with standard error bars. Subject 3 is not included in the lower plot due to lost timing data. Subjects 1 and 2 do not have time data in the Hand Free condition because they did not perform any successful lifts.

Overall, grip strength was decreased when using the HandSOME, but this reduction was not statistically significant (p=0.17). On average the subjects lost 3.7 N of grip force with average grip strength of 29.9±1.9 N for hand alone, and 26.2±1.8 N with the HandSOME. This decrease in grip force was comparable to what would be predicted by calculating the extension torque applied to the hand by the springs. The aperture during testing corresponded to approximately 30 degrees of extension, which puts the extension torque at 0.12 Nm (2 springs), 0.18 Nm (3 springs), 0.24 Nm (4 springs), and 0.30 Nm (5 springs) for Theta=0. For the one subject who used 3 springs and Theta=10 deg, the torque was 0.23 Nm. Assuming an approximate finger length of 0.09 m, the average force lost from the springs would be 3.83 N.

Although all subjects had a large comfortable range of motion with HandSOME, no subject attained 90° of MCP extension as was the goal when determining the number of springs during fitting. This was most likely due to increased hypertonia after a period of hand use. Rapid changes in tone levels could also explain why hypertonia measurements at full extension matched assistance torque for only half of the subjects. Hypertonia could have decreased due to the stretches performed during the tone measurements, or increased due to the unassisted range of motion testing. Although springs could be added or removed as needed to compensate for these fluctuations, we elected to not adjust the number of springs after the initial fitting period to properly evaluate the fitting procedure we developed.

In the unassisted hand functional testing, subjects were allowed to compensate by pushing their hands over the blocks, which allowed some subjects with little or no volitional extension to grasp some of the smaller blocks. Although this created some discrepancies between the range of motion data and the implied range of motion of the functional testing, this method allowed for the most realistic evaluation of real world use of the affected hand. The subjects did not use this compensation method with the HandSOME device.

Some decrease in grip force was expected since the hand was not fully closed during grip testing, resulting in extension torques from the springs that would reduce grip force. The estimated theoretical lost force (3.83 N) was approximately equal to the measured force lost (3.7 N). However, three subjects actually showed increased grip strength with the HandSOME, which could be due to a better hand posture when the springs were applied. Nevertheless, decreased grip force did not affect the functional lifting task with HandSOME, as in all cases a failed attempt was due to inability to open the hand wide enough for the object and not due to difficulty maintaining a large enough grip force.

4.   USE WITH THE ARMIN III REHABILITATION ROBOT

The HandSOME device was integrated with the ARMin III robot to allow for functional task training in the robot. The HandSOME encoder was connected into the ARMin III data acquisition system and a wrist platform was created to allow for adjustment of the device position. The wrist component was designed so that the HandSOME device could

be flipped forward to make it easier for the subject to be fitted into the ARMin device as shown in figure 2.8.

Figure 2.8 showing the interface of the HandSOME device with the ARMin III robot and the ability of the device to fold forward to make it easier to get patients into the robot.

The ARMin III software was also edited to include the movement of the virtual hand and the ability for object manipulation. Further detail on the functional training software with the HandSOME device can be found in Chapter 3.

5. HANDSOME DEVELOPMENT FOR HOME USE

Initial testing with the HandSOME device implies that it would help helpful for in therapy in the clinic. However, the use of the HandSOME device in the home environment both for training and as an orthotic would allow for increase therapy intensity with reduced cost. A wireless gaming system would create a motivating program for home therapy with the HandSOME device. One of the main issues for home use was making the device easier for patients to put on.

Home HandSOME Protocol

Putting on gloves and hand devices is typically very difficult for stroke survivors due to distal finger curling from hypertonia in the finger flexors. It can be very frustrating and time consuming for patients to put devices on their affected hand. This frustration may lead to decreased use of hand device. In addition to reducing effort, several considerations must be made to ensure that the device is fit properly at home to avoid applying abnormal joint torques to the hand. This is the reason that a soft prefabricated wrist brace is used with HandSOME device for all subjects. Although some subjects may not need a wrist brace for stabilization of the wrist into a neutral position, the wrist brace also helps to fix HandSOME's position on the patient's hand using a Velcro strap. In the first session a clinician will fit the HandSOME size parameters to the patient's hand, which minimizes the number of adjustments needed before use. A protocol was created to help patients overcome the issues of distal hypertonia to don the HandSOME device using a table to hold their fingers stretched out.

HandSOME Donning Protocol

1) Put on the wrist brace with the support running through the arch of your palm.

2) Align the center of your knuckles with the center of the encoder of the HandSOME device (as shown in the Fig 2.9) and attach the Velcro to the wrist brace to secure this alignment.
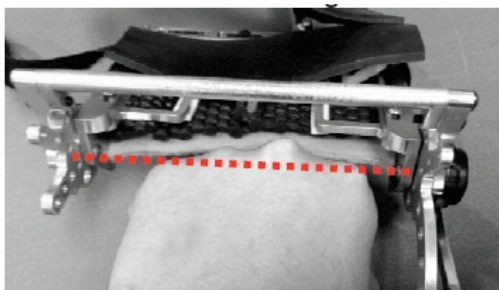
Figure 2.9. Shows the alignment of the HandSOME device with the knuckles of the hand. The red line shows the proper alignment of the device.

3) Stretch out your fingers on a table in front of you. Slowly pull your hand back to the edge of the table and attach the first strap (shown in Fig. 2.10 C). Pull your hand back further off the table to attach the second strap (shown in Fig. 2.10 C).
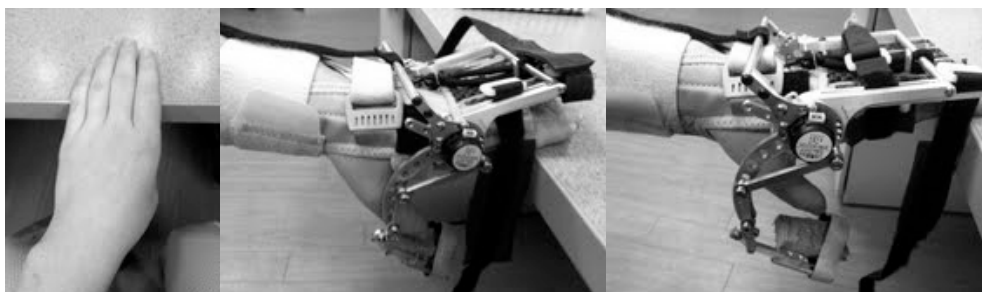
Figure 2.10 A. Shows what the hand is doing without the device on. B and C show the process with the HandSOME device on.

3) Attach the thumb strap.

4) Open and close the device with your unaffected hand to make sure that the system is fitting comfortably.

<u>Hardware for wireless transmission</u>

The HandSOME device was equipped with a potentiometer to measuring the absolute position of the hand during grasp. This signal was sent wirelessly to a computer using the Digi International XBEE system. The XBEE system uses radio signals to transmit the data to the XBEE explorer, which is placed in the USB port of the receiving computer. The XBEE system weighs 88g (3ozs) and attaches to the wrist brace using Velcro. A detachable plug connects the potentiometer to the XBEE system. The system uses a lithium ion battery that was tested running the XBEE system for over 15 hours.

Figure 2.11. The image on the left shows the independent parts of the system including the red XBEE explorer that plugs into the USB port of the computer. The image on the right shows the system on a person.

<u>Game Training Software</u>

The HandSOME gaming software was created to provide motivational training starting with grasp position control at different range of motions and then dynamic movement training.

The game was created using the python based Panda3D gaming platform for interactive training in addition to real world object training. In the game the position of the fingers controls the position of a squirrel on the screen and the user is asked to collect acorns for points and avoid the cats that want to eat the squirrel. The position of the subject's hand in grasp, the number of cats, and acorns hit are recorded by the program. Hitting a cat temporarily reduces the speed of the squirrel, and the number of cats hit is also displayed to encourage the subjects to avoid the cats.

The first part of the game is determining the spring assistance setting that the subject should use (Figure 2.12). The patient starts with their hand closed and attempts to relax and open their hand to collect the acorn. If the squirrel loops across the screen twice without collecting the acorn the subject is told to click 'Pause', add a bungee cord to increase the devices assistance, close their hand, resume the game, and try again.
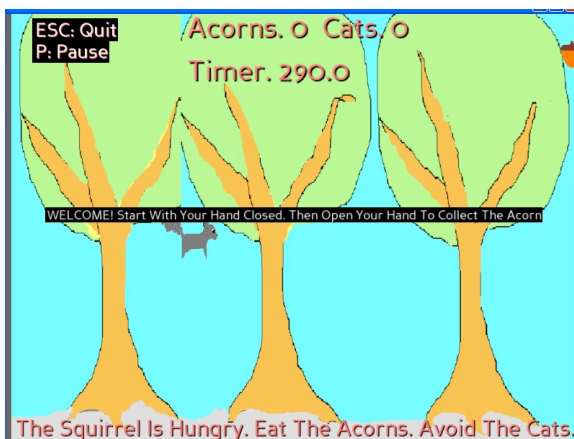
Figure 2.12 Initial game interface for assistance torque determination.

After the subject has determined their assistance setting the subject is asked to maintain a grasp position to collect acorns at different levels of grasp (Figure 2.13). The first set of acorns is near the bottom of the screen and the subject must maintain a very closed hand position. After the subject has collected 10 acorns a new row of acorns appears at a higher position on the screen. The subject must open their hand and maintain that finger position to collect 10 acorns. This process is repeated once more with a higher acorn row position.
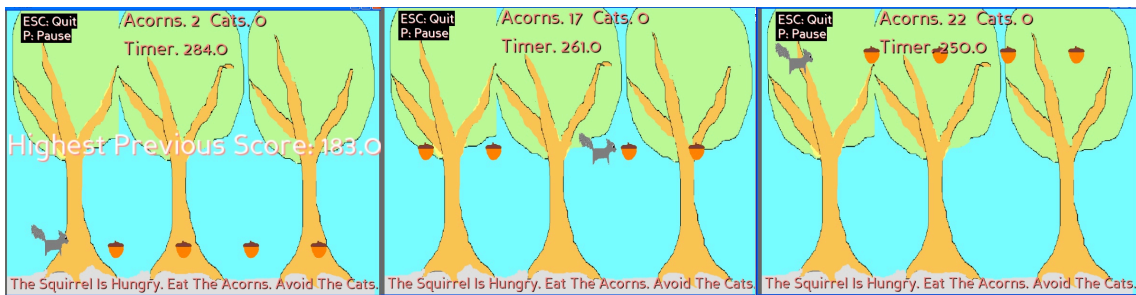
Figure 2.13 The three game levels requiring constant grasp position.

After the subject has collected all of the acorns in the constant grasp levels the dynamic mode starts. The subject must open and close their hand to collect the acorns and avoid the cats as shown in Fig. 2.14.
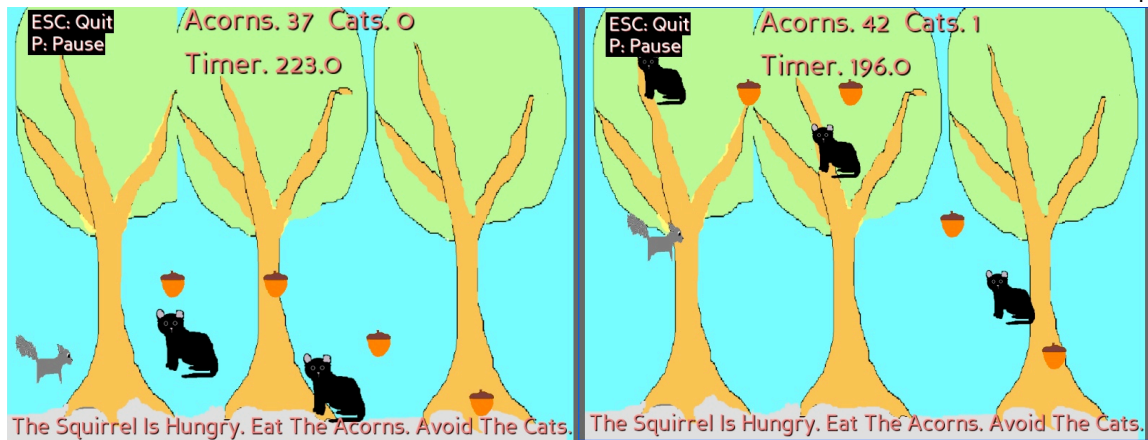
Figure 2.14 The two dynamic mode levels where the subject must open and close their hand to collect the acorns while avoiding the cats.

The final dynamic mode level (right image in Figure 2.14) increases in difficulty after two successful rounds. The cats begin to move vertically across the screen and loop around creating a dynamic avoidance task.

Case Study

A single stroke subject was tested to examine the possibility of the device to be used in the home environment. The subject was trained on how to don the device and start the program. For pilot testing the subject was asked to use the game for 5 minutes under observation at the National Rehabilitation Hospital. Two sessions were used, one week apart. The first session was focused on training device fitting and getting the subject acclimated with the program.

In the first session the device was donned with the assistance of a researcher and then the subject played the squirrel game for 5 minutes obtaining a score of 103 acorns. Feedback

was positive and the subject did not have any comments on the device or game. In the second session, one week later, the process for donning the device was demonstrated again and then the subject was asked to take their time and don the device with only verbal guidance by the researcher. The subject was able to don the system in 5.5 minutes, 1.5 minutes of which was devoted to putting on the wrist brace. The subject then started, and played the game for 5 minutes and achieved a score of 121 acorns. The subject said that putting on the device took a very long time, but thought that it the time might decrease with repeated use. In both sessions the subject required two bungee cords for assistance.

6. CONCLUSIONS ON THE HANDSOME DEVICE

The HandSOME device can assist stroke survivors regain functional grasp ability. The newest version of the device is very low weight, which should allow for arm transport with the device, ADL use even in subjects with shoulder weakness, and minimal impact on the ARMin III robot motor strength. In summary, the general benefits of the device are: 1) passive, lightweight, wearable hand rehabilitation device, 2) small device profile with no internal grasp structures for use in ADL, 3) a linkage for improved coordination of the fingers and thumb, 4) allows for nearly full range of motion in pinch-pad grasp, and 5) adjustable torque profile and magnitude to best match the subject's hypertonia for accurate and optimal compensation. Subjects showed large increases in active range of motion with the device as well as increased ability for functional grasp of objects. This improved ability should help encourage stroke survivors to use the affected limb in everyday activities, which may lead to improvements in hand function without the

device. The HandSOME device was successfully implemented with the ARMin III robot and pilot testing of the HandSOME device for independent use was promising. The system for wireless transmission of data and the game development worked well and our subject had no complaints about the game. However, the time required for donning the current system would likely limit use in the home environment and further design improvements may be needed.

CHAPTER 3. ROBOTIC TRAINING MODES FOR STROKE REHABILITATION

Abnormal interjoint coordination is commonly observed after stroke and in therapy strategies that promote relearning of normal interjoint coordination and movement kinematics may have critical effects on actual real-world use of the limb in ADLs (Lum 2009). Therapies that allow use of compensatory strategies may actually impede this process (Krakauer 2006, Roby-Brami 2003). Therefore, we have developed a therapy method that inhibits compensatory strategies and promotes learning of proper interjoint coordination during reaching movements. The use of the mode to train normal coordination after stroke was tested by training an abnormal coordination pattern in neurologically normal subjects. Some of the following text and figures were previously published in the Journal of Rehabilitation Research and Development (Brokaw 2011).

1. TIME INDEPENDENT FUNCTIONAL TRAINING (TIFT)

The TIFT mode was designed for retraining functional tasks after stroke but can be used for training any path. The mode can be controlled by any of the robot joints in any pairing combination. Although all the arm joints could be set as control joints, moving through the path with only the main joints used in the trajectory set as control joints is easiest. Usually, the two joints with the largest range of motion (ROM) during the task are chosen as control joints. For example, to put an object on a shelf, the main two movements are elbow extension and shoulder elevation. These are the joints that would be set as the default control joints for that task. The subject is required to appropriately coordinate the two control joints to progress along the trajectory. Haptic walls are provided at the

control joints to constrain the subject to the proper interjoint coordination between the shoulder and elbow. If the proper shoulder-elbow coordination is performed, these haptic walls allow the subject to move through the trajectory at his or her own pace and without resistance or assistance from the robot. In the shelf task, the shoulder must be elevated and the elbow extended at the same time for proper completion of the task. The robot will not allow advancement in the trajectory if the subject first raises his or her shoulder and then extends his or her elbow in sequence. Advancement is also not allowed if simultaneous shoulder elevation and elbow flexion occurs instead of elbow extension. If the ratio of shoulder elevation and elbow extension is within a desired window (desired ratio plus or minus a deadband), movement is allowed and the haptic walls guide the joints toward the correct ratio. In this way the TIFT mode requires the subject to actively produce the proper joint coordination to move through the trajectory. While the subject navigates the two control joint trajectories, the other joints are moved along their desired trajectories with a proportional-derivative (PD) position feedback controller. Advancement at all joints, control and slaved, is coordinated through a global advancement parameter that assures normal limb kinematics during the task.

Trajectory Progression with TIFT

Joint angle paths for all joints move through the task and then back, with the same coordination, to the starting position as one repetition. The angle values over time for each joint were normalized between 0 and 1 to make the ROM of the joints easily variable with gains. The time dimension of these paths was also normalized between 0 and 1.

The global variable G is defined as the current point and is the fraction completed of the trajectory. This variable begins at 0 and moves to 1 as the subject returns to the initial position. For all joints, the current G value and the target joint angle paths determine a reference angle for each joint (q_{ref}). The uncontrolled joints are servoed with a PD controller to q_{ref}. For control joints, haptic walls in front and behind the q_{ref} are constructed with a 4° deadband. Therefore, for a constant G, each control joint has 4° of free play before hitting a wall. This 4° deadband is wide enough for smooth unrestricted movement through the path when the subject is producing the correct joint coordination, but it will still keep the subject close to the correct joint kinematics when he or she is maneuvering through the joint space walls. The current position (q_{act}) is used for calculating the single joint advancement variable, g, and provides a measure of that joint's location relative to its desired path. This calculation is not straightforward, as shown in Figure 3.1.
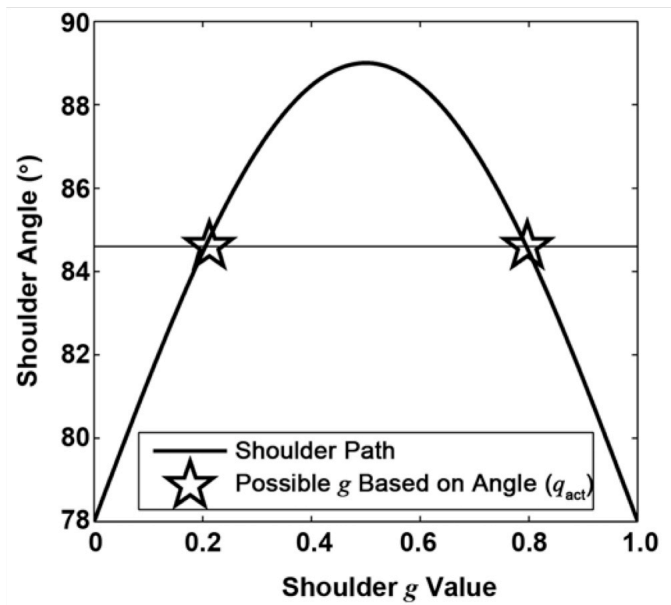
Figure 3.1 shoulder trajectory in shelf path: demonstration that g (single-joint advancement variable) is not unique for given shoulder joint angle (q_{act}).

Because of possible reversals in the joint path, a value of q_{act} can be associated with multiple g values. Therefore, the method relies on a linear approximation to calculate Δg as a function of q_{act}, q_{ref}, and the joint angle, for a 2-percent advancement in the local g value ($q_{refplus}$). Figure 3.2 illustrates this algorithm and describes the special case in which the joint path reaches a plateau.
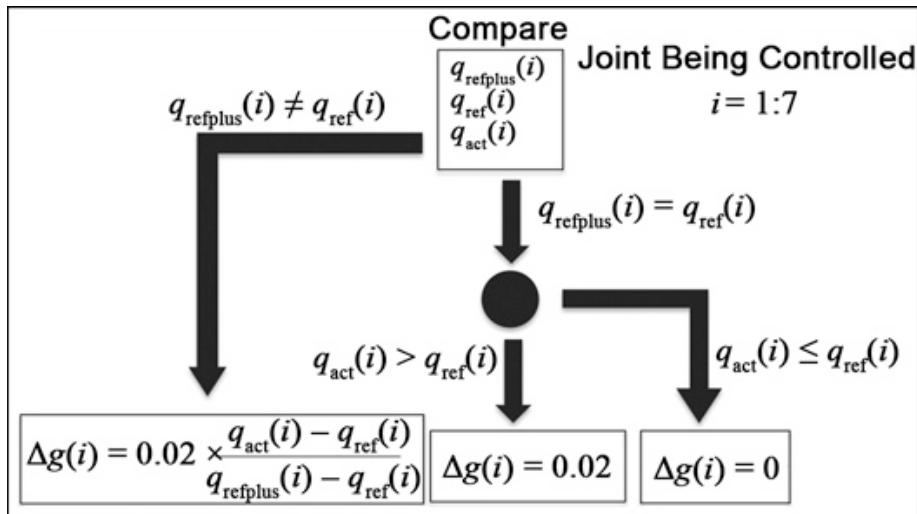
Figure 3.2 Algorithm for calculation of change in single-joint advancement variable Δg. q_{ref} = reference joint angle on path, $q_{refplus}$ = reference joint angle for 2 percent advancement in g, i = robot joint.

The change in G is determined by adding the minimum progression of all of the control joints (Δg) along the trajectory. The addition of the smallest Δg to obtain the new G guarantees that all the joints must progress together to complete the task. The new G establishes new reference joint angles for all joints (q_{ref}). Negative Δg values are set to 0 to prevent subjects from moving backward along the trajectory. When the subject returns to the initial position, the G value becomes 1 and is then reset to 0 so the subject can repeat the pattern as many times as desired.

Boundary Walls for Trajectory

We used the g value of each control joint to determine the locations of boundaries for haptic walls in front and behind q_{ref}. A deadband of 4° provides a joint-space channel that

the subject can move through to complete the trajectory without hitting a wall. The joint walls were defined with exponential stiffness as described in Figure 3.3, where τ is the boundary wall torque, C is a constant that determines the stiffness of the wall, and D is the deadband angle. The wall stiffness constant, C, was tuned for each joint to ensure proper feedback and adherence to the 4° deadband ($C_{shoulder} = 1.5$ deg^{-1}, $C_{elbow} = 1.2$ deg^{-1}). Slaved joints were given a deadband of 0.4° so some compliance would exist in the joints but they would still track their trajectory according to the progression of G. We applied an additional gain factor to convert the exponential terms into the torques applied by the motors ($K_{shoulder} = 1.5$ Nm, $K_{elbow} = 1$ Nm). The torque applied when the subject is moving 1° beyond the deadband of the shoulder is 3.48 Nm in the TIFT mode. This torque provides a solid barrier to keep the subjects within the desired joint position range.
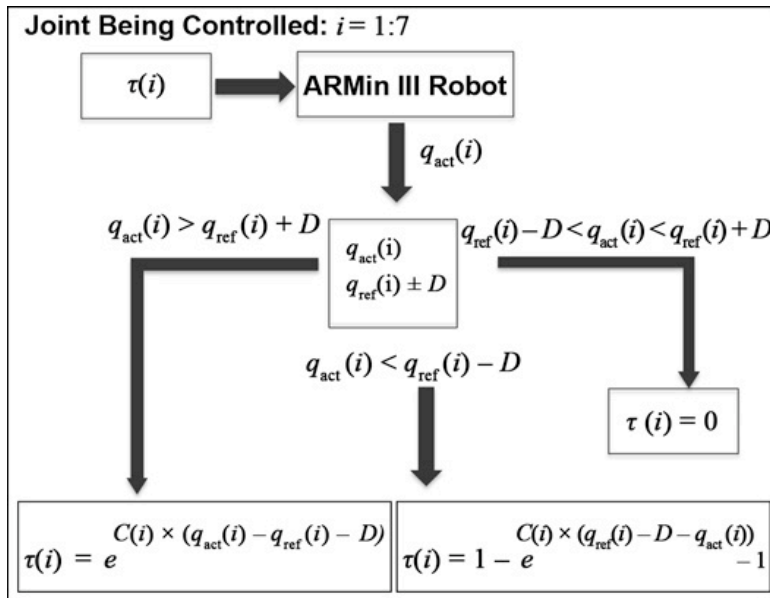
Figure 3.3 Torque applied to ARMin III robot control joints based on their position relative to reference position on trajectory. τ = torque applied by robot, q_{act} = current joint angle, q_{ref} = reference joint angle, $q_{refplus}$ = reference joint angle for 2 percent advancement in g, D = deadband, C = constant that determines stiffness of joint walls, i = robot joint.

<u>Examination of TIFT mode in Neurologically Normal Subjects</u>

Thirty-seven nondisabled subjects were recruited and divided randomly into the three training groups: TIFT, visual demonstration, and TD training. All subjects underwent two time-dependent movements through the desired path with the subject's arm passive in the robot; they then performed a recall of the path with no robotic assistance so we could measure the subject's initial performance of the task before training. Subjects performed 8 blocks of 10 repetitions of the task training with recall testing and 1 min of rest between each block. We gave no feedback to subjects about their performance quality during

recall or training. We did not use the ARMin III visual display because meaningful performance feedback of adherence to a complex 3-D path is difficult to provide in a two-dimensional display, and graphical feedback could increase visual dependence in learning the path.
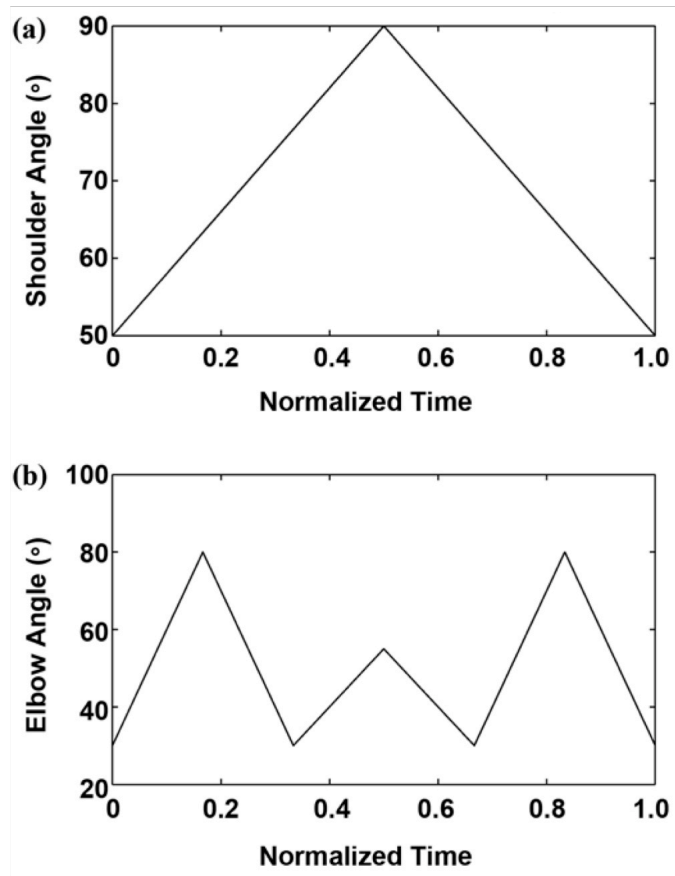
Figure 3.4 Joint paths used in motor learning experiment: (a) shoulder elevation angle and (b) elbow flexion angle.

We chose the shoulder elevation and elbow flexion/extension paths shown in Figure 3.4, largely because interjoint coordination is known to be impaired between these two joints after stroke. This configuration produced a complex, novel, 3-D movement that would

require motor learning for mastery. Using a novel movement pattern is important for avoiding prior ability so we could demonstrate measurable learning during the training. The main complexity of the path was in the elbow. Three extension and flexion movements of the elbow were performed in each task repetition. However, we made the amount of elbow flexion different between the top and bottom shoulder positions to avoid symmetry that would simplify the task. The arm was positioned at 30° of internal rotation of the shoulder and with the wrist in the neural position. This produced movement that was not restricted to a single plane and further complicated the trajectory.

2. ARMIN III ROBOT

All training and recall testing was performed in the ARMin III rehabilitation robot (Figure 3.5). The ARMin III is an exoskeleton robot with six active DOFs, which assist the patient with 6 degrees of freedom of the arm (3 shoulder torques, elbow flexion-extension, supination-pronation, wrist flexion-extension). The ARMin can measure the angle and apply torque directly to each of these joints. We engaged the compensation for the robot's weight and viscous friction to decrease the impedance of the robot. Gravity and friction compensation for the robot arm is vital for minimizing the interaction forces required to move the robot in the "free" mode used in the recall trials to evaluate learning of the trajectory. A detailed description of how gravity compensation for the robot was calculated can be found in Appendix 1. Although the ARMin III has a visual interface designed for patient feedback, as shown in the background of Figure 3.5, we did not use this interface in this study.

Figure 3.5 ARMin III robot and passive hand device, HandSOME, being used in functional shelf task in time-independent functional training mode.

In the TIFT mode, the desired joint rotation direction is known at each point in the trajectory. This directional information allows the robot to provide feed-forward static friction compensation in addition to gravity and viscous friction compensation. The robot provides a small torque in the desired direction approximately equal to the static friction value determined experimentally. Although this torque does not move the robot, it decreases the amount of force required to initiate movement at the joint. This feed-forward compensation also makes it harder for the subject to move in the direction opposite of the desired direction; static friction is effectively doubled in the opposite direction. When the joint velocity is greater than a small value, this torque is set to zero and the viscous friction compensation is engaged. A complete description of this method and experimental determination of static and viscous friction of the ARMin III robot joints has been reported elsewhere (Nef 2009). The torque required to initiate movement at the elbow flexion and shoulder elevation joints of the robot was 0.39 Nm (Nef 2009).

3. TD TRAINING, VISUAL DEMONSTRATION, AND RECALL TESTING

Two training modes were developed in conjunction with TIFT to examine the effectiveness of TIFT. TD training, visual demonstration, and TIFT were used as the training methods. TD training is commonly used for robotic therapy. The robot moves a subject's arm through the task using a PD feedback controller tuned for each joint so that small errors occur in joint positions relative to the ideal reference trajectory ($K_{\text{shoulder}} = 62$ Nm/deg, $K_{\text{elbow}} = 5$ Nm/deg). The subject is asked to actively move along with the robot through the task. In visual demonstration, the subject stood behind the robot, as close as possible to the perspective of the stand-in person in the robot. The subject was then asked to watch the stand-in's arm as it was moved through the path by the robot. The subject was told not to move his or her arm as he or she learned the movement. The stand-in was used for visual demonstration training because it was difficult to visualize arm joint position without a human arm in the exoskeleton robot. The robot used a stiff PD controller to move along the trajectory with minimal kinematic error, so the stand-in did not have a noticeable effect on the trajectory. Therefore, the visual image of a human arm moving through the trajectory was consistent across the three training groups. As in the study by Liu et al., we used the visual demonstration group to examine the effectiveness of visual demonstration on learning a novel task for comparison with the haptic robot-assisted modes that provide both robotic guidance and visual demonstration (Liu 2006).

For all subjects, trajectory recall was tested before and after each training block. In the recall phase, the subject was asked to repeat the trained shoulder-elbow trajectory three times in the robot while the other joints were locked in their appropriate positions. The

elbow and shoulder of the robot were in "free" mode with minimal resistance to movement. The robot provided the best possible "free" mode by compensating for the robot's weight and viscous friction during recall. The most back-driveable joints (shoulder elevation, elbow flexion/extension) were chosen for the trajectory. Although robot inertia would affect the movements, the subjects controlled the speed of the recall movements and moved the robot at a self-selected velocity, which minimized the influence of robot inertia. Haptic walls were placed 1° beyond the ROM of the shoulder in both directions. This kept the subjects within the ideal ROM of the shoulder and made for easier analysis of data. In all the modalities, a PD controller moved the robot to the initial position of the task before starting training or recall.

In both the TD training and visual demonstration modes, each repetition was completed in 12 s. TIFT mode subjects were informed if they were going slower than the 12 s required to complete a single-task repetition in the TD training mode, to avoid any possible advantage they could have from extended time learning the path. On average, the TIFT movement time was 13.1 s and not significantly different from the 12-s time in the TD group ($p = 0.093$). The 12-s path time was used to provide a comfortable and smooth movement in the robot during the training modes. This relatively slow path encouraged similarly slow movement in the robot during recall attempts, which minimized inertial effects. The subject average movement time in recall was 12.25 s, which was not significantly different from the 12-s demonstration speed ($p = 0.605$). For the entire experiment, the only visual feedback received by the subjects was looking at a human arm moving through the pattern (their own arm or the arm of the stand-in).

Data Processing

We calculated three performance metrics for each recall phase: joint error, slope error, and movement variability. Each recall consisted of three repetitions of the movement. The simplicity of the shoulder trajectory results in a unique desired elbow angle for each shoulder position. The shoulder ROM was divided into 1° bins. For each bin, we determined the six time intervals when the shoulder angle was within this bin. The elbow angle was averaged within each of the six time intervals. These six values of elbow angle were then averaged to produce an estimate of the elbow angle associated with the corresponding shoulder angle. This resulted in the phase plane plots shown in Figure 3.6.
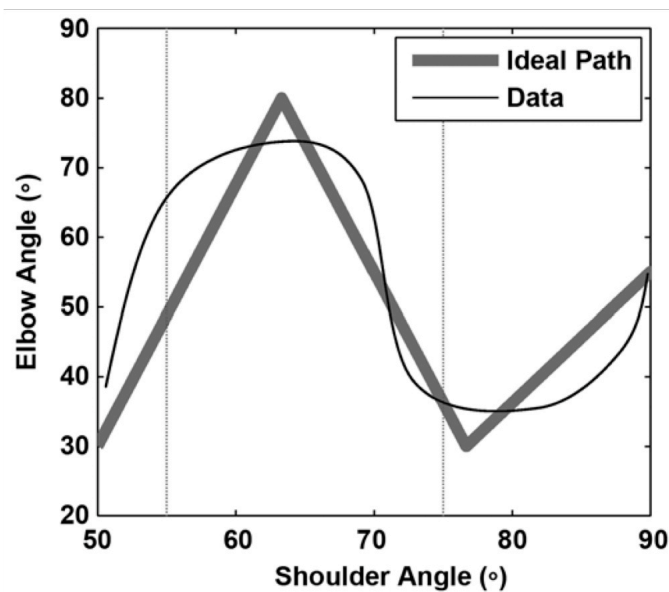

Figure 3.6 Joint coordination pattern of shoulder and elbow in motor learning testing. Thick gray line is desired reference trajectory and thick black curve is an example actual trajectory. At shoulder angle of 55°, elbow should be at 49°. However, elbow is actually about 65°, an error of 16°. However, when shoulder is at 75°, elbow error is nearly zero.

We also calculated the standard deviation over these six elbow angle values, and used the mean of these standard deviations over the ROM of the shoulder as an estimate of movement variability. We then calculated the absolute value of the difference between the ideal reference elbow angle for each shoulder position and the recall elbow angle at that shoulder position. We then added these values across the ROM of the shoulder to provide the area between the reference and actual phase plane plots shown in Figure 3.6. The subject's joint error in the trajectory was obtained by dividing this error area by the ROM of the shoulder. The phase plane trajectory was then divided into three phases with different shoulder-elbow movement ratios. We calculated the slopes of the subject recall data within each phase. We calculated the slope error as the absolute value of the difference between actual slope and ideal slope for the corresponding phase. The mean slope error over the trajectory was the mean of the slope errors over the three trajectory phases. We performed the same procedure on the training data and resulted in average metrics for each training block.

We used univariate analysis of variance (ANOVA) to test for group differences at baseline in age and the performance metrics and chi-square tests to test for group differences in sex. We used repeated measures ANOVA (within-subjects factor of block, between-subjects factor of group) to assess group differences in the pattern of learning across training as well as recall trials.

Results

Thirty-seven subjects completed the training. Outliers were defined as those subjects with baseline performance errors greater than the upper quartile $+ 1.5 \times$ interquartile range, or

less than the lower quartile − 1.5 × interquartile range. Two subjects had very large initial recall errors and were determined to be outliers. Deletion of these two poor performing subjects significantly improved the between-group balance in baseline performance. The following analysis is limited to the remaining 35 subjects (12 in the vision group, 14 in the TIFT group, and 9 in the TD group). The mean age was 33 ± 13 years, and ANOVA found no group differences in age ($p = 0.198$). The ratio of male to female subjects did not differ from a 1:1 ratio in any of the groups ($p > 0.1$). Two subjects were left-hand dominant and one subject was ambidextrous.

Figure 3.7 shows the typical change in the training pattern in a TIFT subject from the first to the eighth block. In the first block, the subject got stuck in the path repeatedly, and two distinct paths were visible for different directions of movement, showing that the subject was relying heavily on the walls. However, in the eighth block, the variability had decreased and the movement had become smoother. Repeated measures ANOVA of TIFT and TD training data showed a significant group × block number interaction in error ($p = 0.002$) and variability ($p = 0.043$).
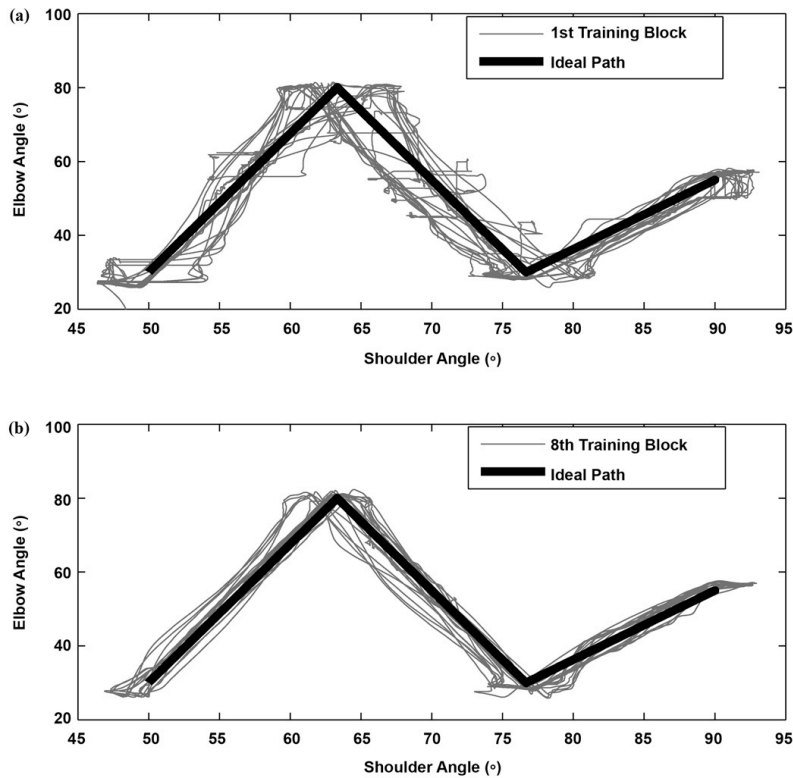
Figure 3.7 Joint coordination pattern of shoulder and elbow during TIFT in a typical subject. The trajectories were disjoint in the first training block, but improved in smoothness by the last training block.

Subjects who received TIFT had significant reductions in error ($p < 0.001$), while TD trained subjects did not reduce error during training ($p = 0.758$) (Figure 3.8(a)). Movement variability decreased significantly over training in both the TIFT ($p = 0.009$) and TD training modes ($p = 0.02$). Mean reductions in error and variability in the TIFT group were 18.7 and 20.9 percent, respectively, while mean reductions in error and variability in the TD training group were 0.48 and 23.4 percent. For slope error, the block factor and the group × block interaction were not significant ($p > 0.6$).
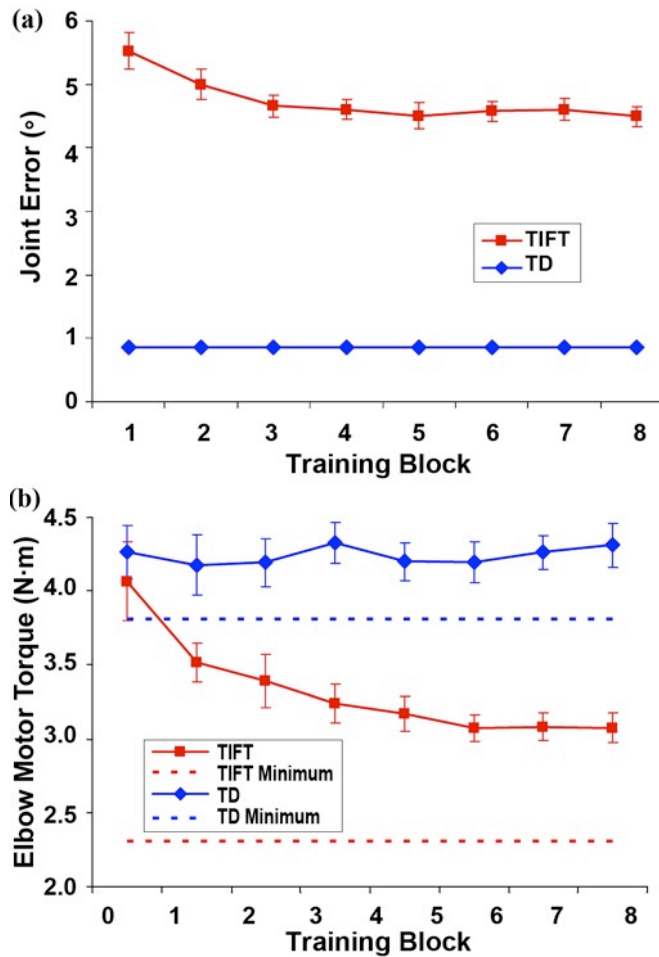
Figure 3.8 (a) Mean error reductions during training blocks for time-independent functional training (TIFT) and time-dependent (TD) groups with standard error bars. Joint error decreases over 8 training blocks in TIFT subjects, but is unchanged in TD subjects. **(b)** Mean elbow torque applied by robot during training blocks for TIFT and TD groups with standard error bars. Minimum possible torque for TD is shown, which is elbow torque required to move through path without human arm in robot. This corresponds to best possible performance in TD training mode. Minimum possible TIFT value is also shown, which is applied torque if subject moves through trajectory perfectly without hitting any haptic walls.

A similar result can be seen in the robot-applied elbow guidance torque during training (Figure 3.8(b)). The mean elbow torques for the TD and TIFT modes were not significantly different for the initial passive movement trials ($p = 0.997$) or in the first training block ($p = 0.564$). However, the pattern of change in elbow torque across training blocks was significantly different between groups (group $\times$ block number interaction, $p < 0.001$). The applied torque decreased significantly across blocks in the TIFT mode ($p < 0.001$), but not in the TD training mode ($p = 0.667$). Applied elbow torque during passive movement was 5.1 ± 0.2 Nm in the TD training group, significantly greater than during the first training block ($p = 0.02$), demonstrating that subjects were attempting to move with the robot during the TD training. Because the TD subjects were trying to move with the robot, one would expect a reduction in applied elbow torque as they learned the trajectory. The minimum possible robot-applied torque for the TD training mode is equal to the applied torque without a subject's arm in the robot. This represents the best possible subject performance, when the subject moves along with the robot perfectly and no interaction forces are applied between the robot and human. However, the TD group did not show any decrease in torque toward this minimum value during training. The minimum possible elbow torque value for the TIFT is the torque the robot applies to compensate for robot weight and friction when the subject moves through the path perfectly without hitting the haptic guidance walls. TIFT subjects showed a steady decrease in robot-applied elbow torque across the training blocks, although they did not reach the minimum torque value. We did not examine shoulder torque trends because of changes between subjects in the spring and cable system that assists with gravity compensation. The spring parameters are incorporated into the

shoulder motor's gravity compensation algorithm, so the motor torque applied to each

subject differed based on the specific spring parameters used during testing (Nef 2009).
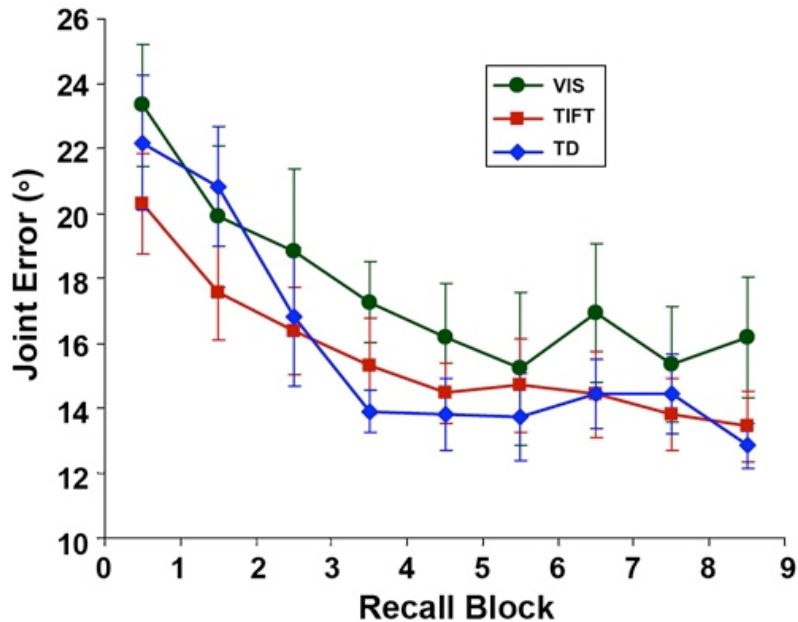
Figure 3.9 Joint error reductions during recall blocks with standard error bars. Significant

learning was present in all groups, but no group differences were present in learning rates

or amount of error reduction.

Initial recall data showed no group differences in baseline error values ($p = 0.36$). Figure

3.9 shows the learning curves for the three groups in the joint error metric. Mean

reductions in joint error between the first and ninth recall tests across all subjects was 35

percent. We performed a repeated measures ANOVA to determine group differences in

the pattern of learning over the nine recall blocks. The block factor was significant in

joint error ($p < 0.001$), slope error ($p = 0.018$), and variability ($p < 0.001$), indicating that

all groups improved in all metrics over the course of the recall blocks. The group $\times$ block

interactions were not significant in any of these metrics ($p > 0.2$). This indicates that all three groups learned with a similar pattern.

Discussion and Conclusions

We presented details of the TIFT mode for training of interjoint coordination as well as a motor learning study to provide initial validation of the modality. Over the course of the recall tests, all subject groups significantly reduced joint error, slope error, and variability. However, the pattern of learning did not differ between groups. Thus, all groups performed equivalently in recall despite significantly better error and torque reductions during TIFT than during TD training. Analysis of the training data showed evidence of learning in the TIFT group, as subjects reduced joint error and movement variability in the robot over 80 repetitions. In contrast, the subjects who received TD training did not reduce error during the training. Similar results were seen in robot-applied elbow torque, with significant torque reductions during TIFT but no change in torque during TD training.

Learning the kinematics of a complex novel movement is possibly dominated by vision, because the additional haptic guidance provided to the TIFT and TD groups did not produce measurable benefits compared with only visual presentation of the trajectory. This result is similar to the findings of Liu et al., who reported no difference in learning a 3-D end-point trajectory between visual demonstration and TD training (Liu 2006). The powerful role of the vision system in motor learning is becoming apparent, with studies showing similar brain activation and plastic adaptation between repetitive practice and

action observation (Stefan 2005). Thus, the presence of vision information possibly overshadowed potential differences between the TD and TIFT modes.

Examination of the training data suggests advantages of the TIFT mode compared with the TD training mode, which may lead to improved outcome in stroke populations. TIFT promoted learning, with the error and guiding elbow torque decreasing significantly over the course of the training. In contrast, TD subjects did not vary their movement strategy during training as the error and guiding elbow joint torque remained constant throughout, despite significant learning of the trajectory in recall trials. Because the instruction to TD subjects was to "move with the robot," and the trajectory was complex and novel, one would have expected a reduction of errors and elbow torque during training as subjects learned the trajectory. If common mechanisms subserve motor learning and recovery of motor control after stroke, then a training mode that promotes decreases in training errors with practice would be hypothesized to be more effective in stroke rehabilitation than a mode in which subjects do not change strategy with repeated trials. A second potential advantage of the TIFT is that it allows for much greater kinematic variability during training, which has been hypothesized to have advantages to fixed trajectory robotic training with small kinematic errors (Lewek 2009). Mean errors during TIFT were more than five times larger than those for TD training. While larger errors in the TD training mode could have been achieved with smaller gains in the position feedback controller, this would not likely have promoted the learning seen in the TIFT data. Therefore, TIFT promotes voluntary exploration of a fairly large kinematic workspace, while the robot

rewards correct movements with trajectory advancement and punishes incorrect movements by not allowing advancement.

Despite these potential advantages of TIFT over TD training, our recall data showed that TIFT was not better than TD in promoting learning of a complex trajectory in nondisabled subjects. Furthermore, learning in TIFT was disjointed early in the training, with subjects often hitting the path walls, stopping and trying several strategies before determining the correct shoulder-elbow coordination needed to advance within the path. Nevertheless, for stroke rehabilitation, we believe further study into assistance modes such as TIFT is needed, given the recent negative findings in robots that have used the TD training mode (Horby 2008, Hidler 2009) and the evidence that passive movement training does not improve motor control (Lynch 2005).

4. EXAMINATION OF TIFT MODE IN CHRONIC STROKE SUBJECTS

The previous results showed the potential for the TIFT mode to be beneficial over TD mode training. However, it did not establish any benefits of TIFT mode with stroke patients. End point training, which focuses on the hand position, is commonly used for movement training. However, this mode allows for abnormal joint coordination and for compensatory strategies to complete the tasks. The follow research presents a cross sectional study with chronic stroke patients comparing TIFT and End Point Tunnel Training (EPTT).

End point tunnels are frequently used for robotic training (Kahn 2006, Burger 2000, Banala 2009). An EPTT mode was created for the ARMin III robot to compare to the TIFT mode. Typically endpoint tunnels allow for free range of motion for all of the robot's joints as long as the hand position remains within the tunnel walls. This allows for abnormal compensation movement patterns such as abnormal internal rotation of the shoulder in reach to grasp movements. However, even with these compensating joints locked, it is suspected that stroke subjects could utilize the walls to complete the trajectory with minimal effort at the more difficult arm joint. This compensation strategy limits the mode's ability to retrain normal movements and muscle activations that are key for functional recovery (Krakauer 2006, Roby-Brami 2003). End point tunnels create a continuous barrier in endpoint space, while the joint space tunnel is disjointed as shown in Figure 3.10 and active coordination of the shoulder and elbow are required to continue through the path.
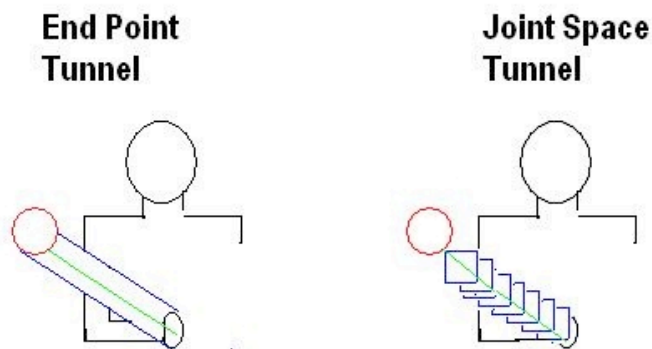

Figure 3.10 Image depicting the differences between end point and joint space tunnels in the end point, hand, coordinate frame. EPTT allows for continuous movement along the tunnel walls, while TIFT does not.

For this study an end point tunnel was created to compare the joint torques of chronic stroke subjects during a reaching movement of the shoulder and elbow. The EPTT and TIFT modes were equalized for deadband and guiding wall force for true comparison of the modalities. For the purposes of this study the reaching movement was limited to movement of shoulder elevation and elbow extension. Shoulder internal and external rotation was locked at 90 degrees and shoulder adduction/abduction was locked at 30 degrees putting the subjects arm comfortably in their lap at the start position. A simple reaching path was created that only involved shoulder elevation from 50° to 90° and elbow extension from 20° to 60° modeled after the functional task of putting an object on a shelf. Although 90° of shoulder elevation is relatively high, since the elbow angle does not go to full extension (0 degrees) it was expected that most of our subjects would be able to complete the trajectory.

EPTT Mode Creation

For a true comparison was very important that the two modalities be completely the same other than the basic difference the mode principles. In order to do this the tunnel walls had to be equalized both for width and stiffness. The forward kinematics and the Jacobian of the ARMin III robot were calculated. This allowed for easy conversion between end point force and joint torque. Since the ARMin III robot is an exoskeleton robot, all of the end point tunnel forces needed to be turned into joint torque forces for implementation.

Since we are only using two joints for the trajectory the conversion to end point was relatively simple. The joint space path was converting into end point space coordinates using forward kinematics shown in equations 3.1, 3.2, 3.3.

$$Hand_x = C_S * L1 + (C_S - C_{EXT} - S_S * C_{EXT} + S_E) * L2 \tag{3.1}$$

$$Hand_y = C_A * S_S * L1 + (C_A * S_S * C_E + (C_A * C_S * C_{EXT} - S_A * S_{EXT}) * S_E) * L2 \tag{3.2}$$

$$Hand_z = S_A * S_S * L1 + (S_A * S_S * C_E + (S_A * C_S * C_{EXT} + C_A * S_{EXT}) * S_E) * L2 \tag{3.3}$$

Where the large letters 'S' and 'C' are for sine and cosine, and the subscript 'A' is shoulder adduction, 'S' is shoulder elevation, 'EXT' is shoulder external rotation, and 'E' is elbow flexion. For example $S_S = \sin(\theta_{ShoulderElevation})$.

These equations were used to equate the joint space trajectory to the end point trajectory. The 1 cm end point tunnel was converted into joint space using the simple inverse kinematics of only the shoulder and elbow, since the other ARMin III joints were locked for testing. This calculation produced an elbow deadband of 1.90 degrees. The shoulder deadband varies between 1.25 and 1 degree due to the change in length to the end point position.

Exponential walls relative to the error in end point space beyond the calculated deadband were used. In this case the error was measured between the reference end point position for the current position in the trajectory and the current hand position. However, for an end point wall the direction of the force is calculated differently to create a continuous

wall perpendicular to the trajectory. First that vector from the current position is found is

found using equation 3.4.

$$\hat{k}(G) = \begin{bmatrix} x'(G) & y'(G) & z'(G) \end{bmatrix} / \sqrt{x'(G)^2 + y'(G)^2 + z'(G)^2}$$ (3.4)

$$b = ((Pt - Pc) \bullet \hat{k}(G)) * \hat{k}(G)$$ (3.5)

$$a = (Pt - Pc) - b$$ (3.6)

Where x, y, and z are the end point trajectories of the hand. Pt is the desired position in

the trajectory, Pc is the current position, and $\hat{k}(G)$ is the unit vector gradient of the

current position of the trajectory. If the end point position is outside of the deadband (|b|

> deadband) the end point force is defined as in equation 3.7. The $\dfrac{a}{\|a\|}$ component of the

force equation makes the force of the wall perpendicular to the trajectory path.

$$F_{sidewall} = K_1 * (e^{K_2(\|a\| - deadband)} - 1) * \frac{a}{\|a\|}$$ (3.7)

K1, and K2 are the stiffness parameters of the walls. The exponential walls allow for

some movement beyond the deadband with rapidly increasing force as error increases. In

order to be like the TIFT mode, a back wall also used to hold the subjects in place if they

started fatiguing. The equation for this wall is given in equation 3.8.

$$F_{backwall} = K_1 * (e^{K_2 (\|b\| - deadband)} - 1) * \hat{k}(G) \tag{3.8}$$

The Jacobian was calculated and used to convert the calculated end point wall torques into joint torques that the exoskeleton robot would apply to implement the end point tunnel.

$$F_{end} = F_{sidewall} + F_{backwall} \tag{3.9}$$

$$Torque_{Joint} = J'*F_{end} \tag{3.10}$$

Equalizing the wall stiffness between the two modes is very important for mode comparison. The two end point tunnel wall gains are related to the joint wall parameters by the length between the motor base and the endpoint. This length is consistent for the elbow but changes for the shoulder. During progression through the path the desired shoulder stiffness for the current position in the trajectory was called from a stored variable.

Trajectory progression with the EPTT mode is different from TIFT. In the end point trajectory, the closest geometric location on trajectory is the current reference point. This is shown in the following equations. The vector parallel to the trajectory path from the current position to the desired position is b as defined in equation 3.11.

$$gradvec = \| k(G) \| \tag{3.11}$$

k(G) is the direction vector of the current position in the trajectory. If the gradvec is greater than zero and the dot product between k(G) and b is less than 0 Δg equals the value from equation 3.12. If the gradvec is zero and the dot product is equal to zero the subject is aligned with the trajectory path and the $\Delta g = 0.02$. In all other cases $\Delta g = 0$. This prevents backward movement on the trajectory.

$$\Delta g = \frac{\|b\|}{gradvec} \qquad (3.12)$$

This Δg is added to determine the current G value, which is the subject's location in the trajectory. Like with the TIFT mode, G is reset when $G = 1$.

Testing Methods

Nine chronic stroke subjects were recruited at the National Rehabilitation Hospital in Washington DC. The study was approved by the Medstar Institutional Review Board. The subjects were consented to the study and randomized into two groups, which determined their initial training method. All subjects went through both training modes, but were randomized to equalize the possible effects of fatigue. Group A started with the TIFT training paradigm, while Group B started with end point tunnel training.

The subjects' upper arm and forearm were measured and subjects were asked their approximate weight. These values were used to calculate the forces for arm weight compensation as described in Appendix 2. Subjects were then fitted into the ARMin III robot and tested for comfort and range of motion.

The simplified reaching task discussed previously was used, and subjects were told to only focusing on reaching up to the target. A physical target was placed at the end of the trajectory. The subjects were given the goal to 'move your hand to the target by lifting your shoulder while you extend your elbow at the same time'. This command was the only verbal guidance that was given to subjects if they were having trouble progressing through the path with either mode.

Subjects were initially moved through the path by the robot once and then asked to reproduce the movement one time in recall mode. In recall mode the robot moves the subject's arm to the start position and then releases the control joints with only robot weight compensation and viscous friction compensation. After the recall movement the initial training section began. The following procedure was repeated for both the EPTT and the TIFT modes.

Subjects were asked to do five total repetitions of the movement to the target. Subjects were given a maximum of thirty seconds per movement. Between each attempt, the subject was told to relax while the robot moved the subject's arm through the path two times. This was done to minimize fatigue by providing approximately 24 seconds of rest between movements, and to help with path recall. The first five training movements used 50% arm weight compensation at the shoulder. This was done to minimize fatigue effects while learning how to move through the training path. After five repetitions the subjects were asked to do the movement in free mode and then the process was repeated without

gravity compensation. A paired t-test was used to examine possible differences between the joint torques during progression through the TIFT and EPTT modes.

Results

Nine stroke subjects were consented to the protocol and enrolled in the study. The subjects averaged 52.1 ± 15.5 years old and 4 ± 2.4 years post stroke. The average Fugl Meyer score was 22 ± 8.6. One subject, aged 74 with a Fugl Meyer of 15, was unable to complete the task with TIFT and EPTT even with 50% arm gravity compensation. The subject's average percent complete was 5.9% with EPTT and 4.9% with TIFT, with 50% arm weight compensation the percentage of the reach complete was 9.4% with EPTT and 9.5% with TIFT. The subject started with EPTT mode, so the decrease in ability with unassisted TIFT mode may be due to fatigue. However, it is hypothesized that the TIFT mode will be more difficult for most subjects to complete due to the effects of abnormal muscles synergies limiting the patient's ability to coordinate their shoulder and elbow during reaching movements. This subject was removed from all analysis due to her inability to complete the task with assistance.

The amount of torque applied by the robot during task progression was measured. This is the torque when the subject is successfully moving through the path. The torque applied by the robot will be zero if the subject is perfectly moving through the path. Extension of the elbow is typically the harder joint for stroke subjects with abnormal muscle synergies. This typically results in subjects relying heavily on shoulder elevation to reach toward the target. When subjects rely on their shoulder, the robot applies a force to push the shoulder

down. Both modes, on average, showed this tendency with the average shoulder torque in TIFT mode being 1.13 Nm and EPTT mode 1.77 Nm and no significant difference in shoulder torque ($p = 0.38$). Figure 3.11 shows the average torque profiles of all the subjects and the average absolute value of the torques during progression. Negative torque means that the robot was doing work in extending the subject's elbow, while positive torque means that the subject was on a forward wall and the robot was impeding movement at that joint. There was no significant difference in elbow torque between TIFT and EPTT modes with or without gravity compensation ($p=0.119$). However, the absolute value TIFT elbow torque was significantly lower than EPTT mode ($p=0.035$). Absolute value of torque at the shoulder was not significant ($p=0.092$).
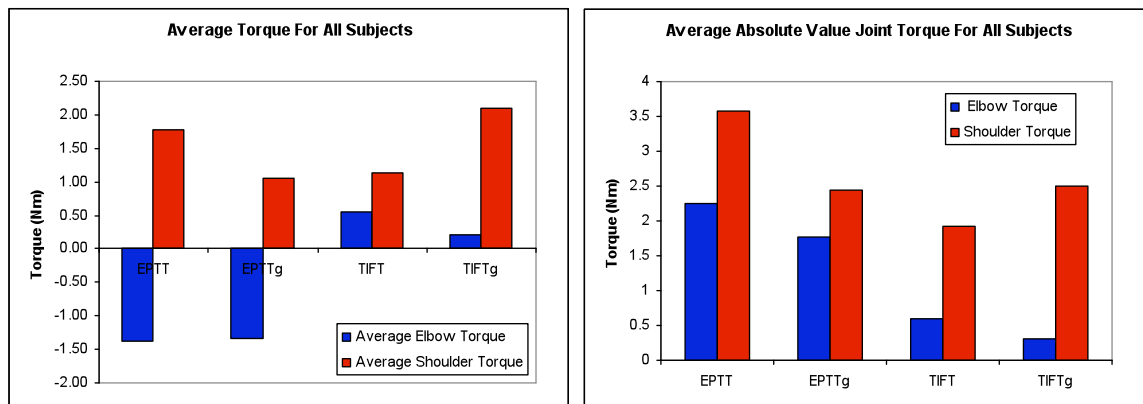

Figure 3.11 The average torque values of the subjects during the different training groups, showing that on average the subjects used the walls for assistance with elbow extension during the EPTT mode. The figure on the right shows the absolute value of torque, which was higher with EPTT.

Two distinctive patterns of movement compensation emerged in the EPTT mode. Five of the nine subjects in the end point tunnel mode were on the upper wall of the tunnel during progression. The average torques for these subjects are shown in Figure 3.11a. For these subjects the average elbow joint torque was significantly larger (p = 0.016) in the EPTT mode, at -3.11 Nm, compared to TIFT mode where the average torque was 0.41 Nm. The EPTT elbow torque with gravity compensation at the shoulder (EPTTg) was also significantly larger than TIFT with gravity compensation (p=0.031) and without compensation (p=0.029). The negative torque means that the wall was pushing the subjects' elbow into extension. In contrast the slightly positive torque in TIFT mode shows that the subjects were actively extending their elbow and even being slightly restricted in elbow extension by the robot. There was no significant difference in shoulder torque between the uncompensated modes for these subjects (p=0.123).

A
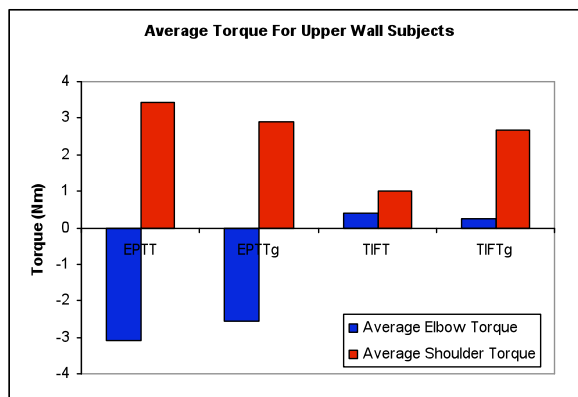
B
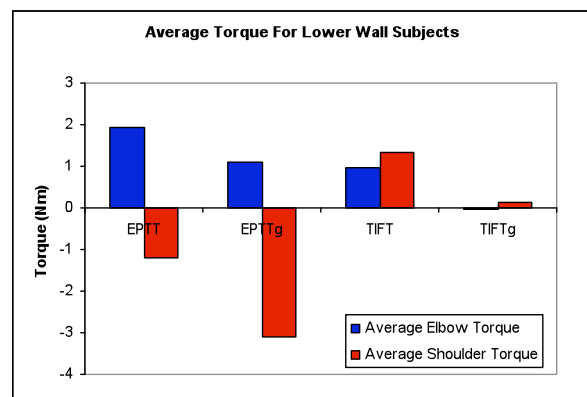
Figure 3.12 These images depict the two different methods used to complete the EPTT mode trajectory. The image on the left (a) shows how subjects used the upper tunnel wall

to assist with elbow extension, while the image on the right (b) shows how the subjects in EPTT mode used the lower wall to assist with shoulder elevation.

Two subjects were on the bottom wall during movement through the EPTT mode and their torques are shown in Figure 3.12b. For these subjects the average elbow torque was 1.93 Nm during EPTT progression, showing that they were leading with their elbow through the path. However, the average torque at the shoulder for these subjects was -1.19 Nm showing that the robot was actively pushing up the shoulder of these subjects during progression. In contrast, in the TIFT mode, these subjects had an average shoulder torque of 1.32 Nm and an average elbow torque of 0.98 Nm. These positive torques mean that the robot was impeding movement through the path to ensure proper joint coordination.

One subject, age 24 with a Fugl Meyer score of 21, preformed very well in the EPTT mode with minimal reliance on the walls. The subject's elbow torques were relatively low as seen in Figure 3.11. The subject did show the trend of upper wall subjects in EPTT mode without compensation, but the torque values are low. The high shoulder torque in TIFTg mode may be learning affect, since TIFTg was trained before TIFT. The trajectories of this subject's movements are shown in Figure 3.11 B. The subject's path appears more disjointed during the TIFT mode without shoulder weight compensation, possibly due to fatiguing.
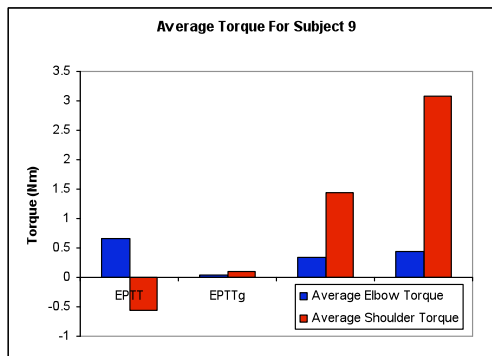
A   B
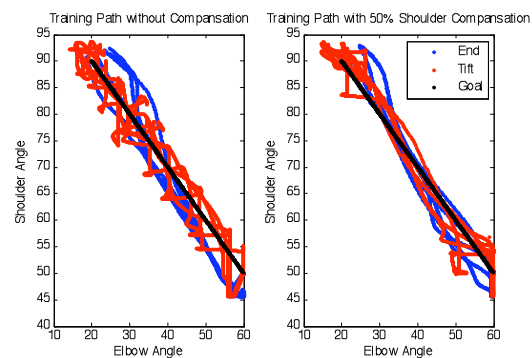
Figure 3.11 Figure A shows the average torques for subject 9. Figure B shows the joint space path for subject 9. The figure shows good trajectory matching in both EPTT and TIFT with 50% shoulder compensation. The tracking is worse for both modes without assistance.

At the shoulder his EPTT torque was -0.38 Nm and in TIFT it was 1.45 Nm. This subject had minimal reliance on the tunnel walls.

The error of the path during training was also measured according to the methods presented in section 3 of this chapter. Subjects in the TIFT training mode were significantly closer to the ideal training coordination ($p < 0.01$) with an average error of 2.97 degrees, while in end point mode the average error was 5.03 degrees. Since the deadband was 1.9 degrees at the elbow and a maximum of 1.25 degrees at the shoulder, the high average error in EPTT mode shows that the subjects were frequently pressing into the tunnel wall during training. Figure 3.12 shows a typical subject that was on the upper wall during EPTT training in the left image (A) and a subject that utilized the lower

wall during EPTT training on the right (B). In both cases the subjects were closer to the target trajectory in the TIFT mode.

A   B
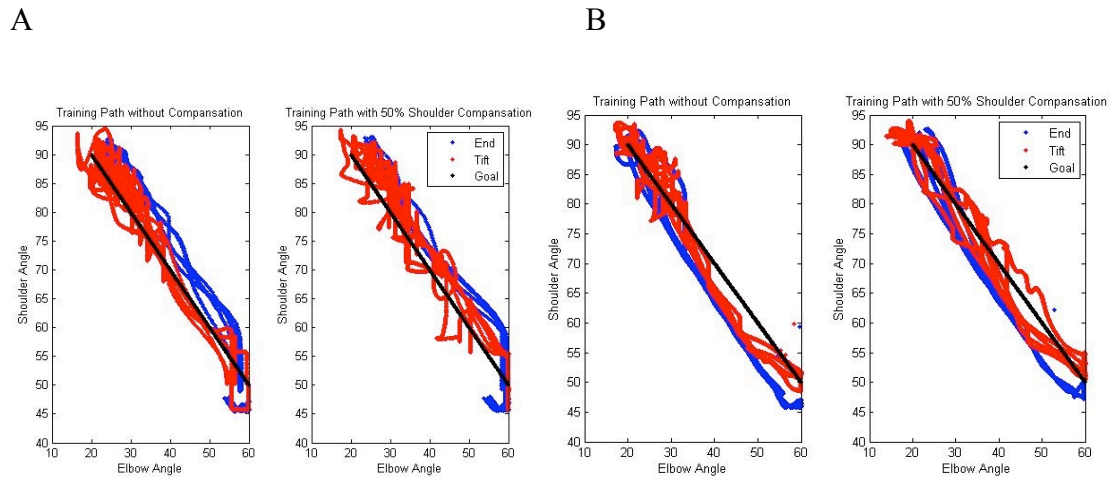
Figure 3.12 Figure A shows the path for subject 7, who used the upper wall for task completion. The subject has a larger error in the EPTT than TIFT mode, but also higher variability in the TIFT mode with gravity compensation. Figure B shows the path for subject 4, who utilized the lower wall for progression through the EPTT mode.

Discussion

Although it was hypothesized that EPTT mode trajectories would be easier to complete with less gravity compensation, the one subject that could not complete the task had relatively similar ability, as measured by percentage of the task completed, between the

EPTT and TIFT modes. The torque results suggest that, on average, the subjects that could complete the task minimized the actual effort and active coordination of the arm joints in the EPTT mode. This would likely lead to decreased improvement from training due to the reduced use of the joint during training. The large training error during EPTT means that the subjects were training on the end point tunnel wall even after five movements in the EPTT mode with 50% arm weight compensation. If more freedom was provided in end point training, such as internal and external rotation at the shoulder with is currently done with some exoskeletons, these results suggest that many subjects would utilize abnormal compensation patterns to further reduce the required active extension at the elbow.

5. CONCLUSIONS FOR TRAINING MODES

Compared with TD training, TIFT has several theoretical advantages: minimally interfering with the input/output map between correct muscle activation and movement, allowing greater kinematic variability during training, and requiring subjects produce proper interjoint coordination to advance within the trajectory. We also observed advantages of TIFT in the training data. Error and assistance forces gradually reduced during TIFT, but no changes occurred in these metrics during TD training. TIFT had lower interaction forces between the robot and human arm than TD and EPTT training, which shows that the human arm was contributing more to the movements during TIFT than during TD training. Although TIFT mode movements are more disjointed than EPTT movements over training it is likely that the movements would become smooth

like was seen with the neurologically normal subjects. These results suggest that TIFT mode would improve on current methods of robotic therapy by increasing the stroke patient's active joint coordination during training.

CHAPTER 4. ARMIN III AND HANDSOME FOR CHRONIC STROKE REHABILITATION

The combination of normal joint movement training in functional tasks and hand function is hypothesized to improve functional use of the affected limb after stroke. Abnormal coordination is commonly observed in hemiparetic arm movements after stroke, and may be the fundamental cause of reaching movement deficits (Zackowski 2004). This can be very disruptive to function in activities of daily life. For example reach to grasp movements, like manipulating an object on a shelf, are often disrupted by the abnormal muscle synergy of simultaneous shoulder elevation and elbow flexion (Sukal 2007). Stroke victims may overcome these deficits through the reliance on compensation patterns, such as excessive trunk movement, for functional activities but studies have suggested that therapy interventions focused on compensation may limit functional recovery (Krakauer 2006). Recovery of proper joint coordination is possible with a focused intervention (Ellis 2005) and may aid in real world use of the limb in activities of daily living (Lum 2009).

The use of robotic devices to treat upper limb movement deficits is becoming increasingly accepted. Although meta-analysis and systematic review of robotic therapy studies have shown significant increases in strength and range of motion, there were no overall advantages of using robots in recovery of activities of daily living (ADL) ability (Prange 2006). These results motivate further analysis of these robotic approaches as well as new untested approaches to maximize restoration of ability in activities of daily living. Although rehabilitation robots have moved away from passive movement therapy due to

studies showing the necessity of subject engagement (Hidler 2009), the type and quantity of assistance that should be provide is still debatable. Since subject ability is often very low it becomes difficult to ensure successful completion of the task without the robot doing all the work. Adaptive control algorithms for the constraint and assistance provided by the robot have also been developed (Marchal-Crespo 2009) to minimize guidance, since excessive assistance may impair task learning (Schmidt 1992). Some groups have used end point tunnels to provide minimal guidance through the desired movement (Kahn 2006, Burger 2000, Banala 2009). However, end point paths do not necessarily insure proper joint coordination through the trained movement, and in many cases allow use of compensatory strategies as shown in Chapter 3.

We have developed a robotic intervention for arm rehabilitation that specifically targets impaired inter-joint coordination by requiring active patient participation in coordinating multiple joints. We implemented this training mode in the ARMin III robot with the HandSOME device for passive tone compensation of the hand allowing for real world or virtual object grasp training. The following paper describes the therapy program designed for functional, patient initiated training. The Time Independent Functional Training (TIFT) modality is for functional training is discussed, and results are presented from a eleven chronic stroke subjects trained across approximately 4 weeks with 1.5 hour sessions delivered twice a week.

1. TIFT CONTROLLER FOR REHABILITATION

TIFT allows patients to learn the desired movement in joint space at his or her own pace while still requiring the patient to actively complete the movement. This system provides guiding joint-space walls to keep the subject close to the ideal joint-space path and holds the subject's arm at the current point in the trajectory if they stop actively producing the required inter-joint coordination.

Three functional tasks: 1) putting an object on a shelf, 2) pouring from a pitcher and 3) sorting objects into bins, were developed for therapeutic use with the ARMin III robot. The combination of the ARMin III and HandSOME devices implemented in the Shelf task can be seen in Figure 4.1a as well as the virtual interface that was used during training in Figure 4.1b. The virtual interface allows for subjects to virtually grasp and release objects during training, for example Figure 4.1b shows the character moving the virtual cup onto the shelf. Compensation for the robot's weight, viscous friction, and static friction were implemented to decrease the impedance of the robot in all modes according to previously reported methods (Nef 2009, Appendix 1).
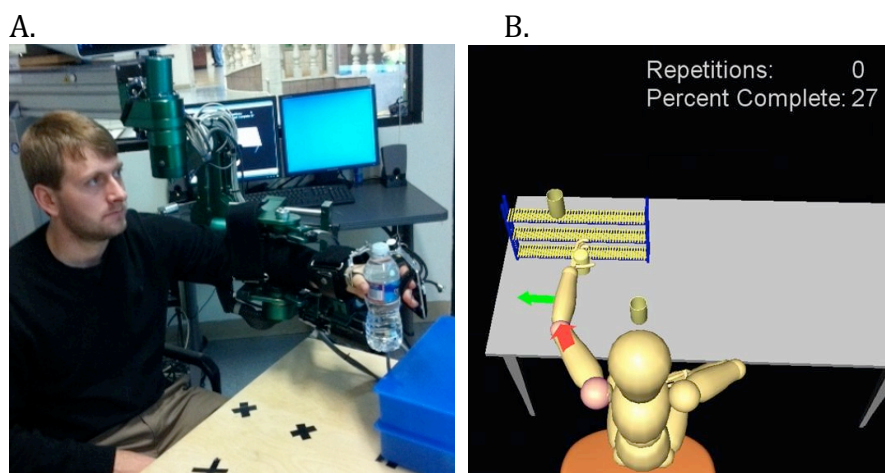
Figure 4.1 A. ARMin III device fitted to a normal subject and in Fig. 4.1B. the corresponding visual interface used for training of the Shelf task. The subject is approximately one quarter of the way through the task, which is lifting and placing the bottle on the shelf and returning your hand to the table.

The Shelf task focuses on correcting the abnormal coordination patterns in the shoulder elevation and elbow extension movement due to the associated abnormal muscle synergy. The path utilized for the Shelf task is shown in Figure 4.2. Figure 4.2a shows the path of the shoulder and the elbow separately with a line indicating the location of the joints at 27% completion as shown in Figure 4.1. Figure 4.2b shows the linear coordination pattern of the elbow and shoulder through the movement, again with a marker denoting 27% completion. The subject starts in the lower right corner, moves up to the left to place the object on the shelf and then back along the same path line to the original position to complete the movement.

A.   B.
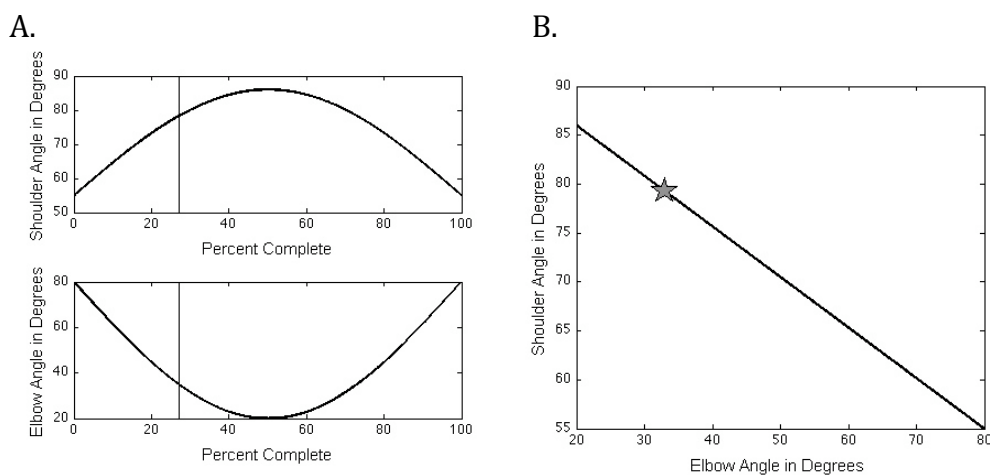
Figure 4.2. The joint movement through the Shelf task and figure 4.2b shows the coordination. The gray vertical lines in figure 4.2a mark the joint angles associated with 27% completion of the Shelf task and the gray star shows the corresponding location on a joint space representation.

The TIFT modality ensures that the subject remains on this coordination pattern shown in Figure 4.2 by implementing joint space walls within a set dead-band around the path and only allowing progression if the arm joints are properly coordinated. If the subject is moving both joints in the proper direction to complete the path, they will not feel any resistance from the robot. However, if the subject attempts an incorrect movement pattern (ie: shoulder elevation with elbow flexion), the robot will prevent movement through the path until there is proper coordination of the two joints. This prevents abnormal compensation patterns and helps break through abnormal synergies. The system also prevents backward movement and will hold the subject in place if they need to rest due to fatigue. Further details on the TIFT modality implementation can be found in the previous chapter.

Two different TIFT settings were used for the task training. In the Shelf task the deadband was set to zero so that any joint space error caused the robot to provide exponential walls that pushed the subject back toward the path. The Sorting and Pouring tasks were implemented with a 2° deadband at each joint. The Pouring task was focused on supination-pronation and shoulder internal/ external rotation, while the Sorting task focused on shoulder elevation and horizontal adduction/ abduction.

Feedback About Goals and Success

A visual interface for therapy was projected in front of the subject to assist with the completion of the movement as shown in Figure 4.1b. The visual interface displays the desired movement of the arm with color-coded arrows placed on the appropriate joints of the avatar. The joint's arrow is green when the subject is properly rotating that joint and red if that joint is limiting the motion. If the subject properly coordinates their arm during the movement, the arrows will remain green throughout the movement. The subject is told to "move in the direction of the red arrow to make it green" in order to complete the task. Subjects were provided with additional feedback about the number of repetitions performed and the current percentage completed of the task. Audio feedback was provided to indicate that the subject had reached the endpoints of the task. An important part of therapeutic intervention is ensuring that the tasks are challenging but doable.

Changing Difficulty in TIFT training

Difficulty of the TIFT tasks can be adjusted through changes in range of motion, the addition of human arm weight compensation, and addition of assistive torque at the most

difficult joint. The mode can also be switched into single joint control for specific focus on target muscles if needed, where the robot will move the other joints through the path utilizing a PD position controller according to the movement of the single controlling joint.

The subjects are able to use real or virtual objects during training. This allows for progression in type of objects that are grasped to practice grip strength and grasp modulation during arm movements. Figure 4.3 shows the range of objects that are used during training with the mode.

Figure 4.3 Image of the objects that are used during training with the ARMin III and HandSOME system. The image shows that the objects varied greatly in shape, size, frailty, and weight.

TIFT Therapy Procedure

The general method used for administering robotic therapy was as follows. An evaluation was done at the beginning of each task, where the robot was set to the highest range of motion (ie highest shelf height or sorting distance) without any added assistance to the TIFT program (ie no subject arm weigh compensation or assistive torques). The subject was then told to make three attempts at the path. If the subject completed only one or none, arm gravity compensation was added until the subject could comfortably train at that task. If 100% arm weight compensation did not allow for task completion, then the range of motion would be reduced. In the Pouring task, constant joint torque assistance was provided to aid in completion since arm weight effects were minimal in that movement pattern.

The most problematic joint in the movement can be determined through examination of the feedback avatar. Through this examination the most challenging joints for individual subjects can be determined and focused on, such as a subject's limitation in the Pouring task being inability to supinate the wrist.

The purpose of the following study was to pilot test the TIFT mode with the HandSOME device in training. This relatively short training study was used to determine subject acceptance of the novel training paradigm and system with the HandSOME device, and any possible improvements in impairment after training.

2. TRAINING STUDY WITH THE TIFT PROTOCOL

Eleven chronic stroke subjects were recruited from the National Rehabilitation Hospital. The study was approved by the Medstar Health Institutional Review Board. Our subjects had an average age of 57 with a standard deviation of 12 years and were an average of 2.9 years post stroke with a standard deviation of 1.9 years post stroke at the start of the trial. Six of the subjects were left affected and only three of the subjects were women. Subjects were trained for approximately four weeks with 8 total sessions, each 1.5 hours long. Before and after the robotic training an occupational therapist administered the Fugl-Meyer, Action Research Arm Test (ARAT), and Box and Blocks to get a clinical evaluation of subject improvements.

Robotic Therapy

A trained physical therapist assisted with fitting subjects into the robot when needed, but a technician administered all robotic therapy. The Ltraj program, shown in Figure 4.4, was started to test the comfortable fitting of the robot and for a measure of current active range of motion. This task only focuses on single joint movement and was worked on for five minutes or less. The subject lifts their arm at the shoulder to lift the ball. After the subject reaches the 25% complete point (shoulder at 90 degrees) at the top of the 'L' the robot holds the subject's shoulder while the subject tries to supinate their wrist to move the ball to the end (10 degrees beyond neutral position). After the subject reaches the end the subject pronates back to the original position and lowers their shoulder. This process

is also repeated with the elbow coming instead of the wrist moving the ball across the screen as the elbow comes in to 90 degrees of flexion.
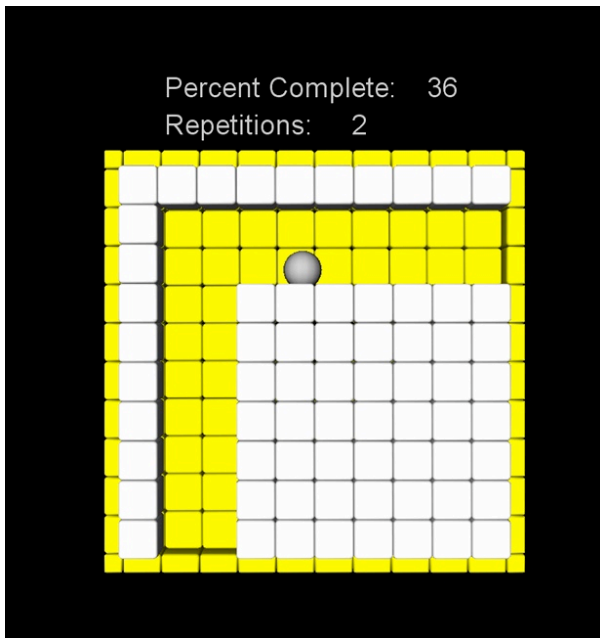

Figure 4.4 Ltraj subject interface for a left affected subject. The patient's hand (white ball on the screen) is brought to the initial position in the lower left of the yellow tunnel. The patient then lifts their shoulder to move the ball vertically; when the patient reaches the bend they rotate their palm up to move the ball to the side.

At the start of each training task, Shelf, Pouring, and Sorting, the stroke subjects were moved through the path three times by the robot to remind the subject of the path. The subjects were then asked to move through the path with the TIFT controller three times before changes were made to the program in accordance with the therapy guidelines. No additional assistance was provided in these evaluation trials, and all training data

presented in the paper is taken from these evaluation movements, where the focus was solely on arm movement and not grasp.

Each task, Shelf Pouring and Sorting, was trained for approximately 20 minutes with 5 minutes of games (ball and labyrinth games reported in Staubli et al (Staubli 2009) with minor changes) played between tasks to break up the training. The high score from the previous game rounds was told to the subject before each game session to provide encouragement to beat their high score. Task training included the grasp of real objects during the Sorting, Pouring and the Shelf task. In later training sessions the subject would grab various objects off a table and move them between locations unassisted during the Sorting task. This helped the subject to learn to coordinate arm speed and hand aperture in the task. Objects varied in size, weight, and fragility to help train the needed changes in movement to the object as well as proper grasp strength control. In the Pouring task subjects practiced pouring from a cup with a relaxed hand so that cup was not crushed. These methods of object manipulation are shown in Figure 4.5.
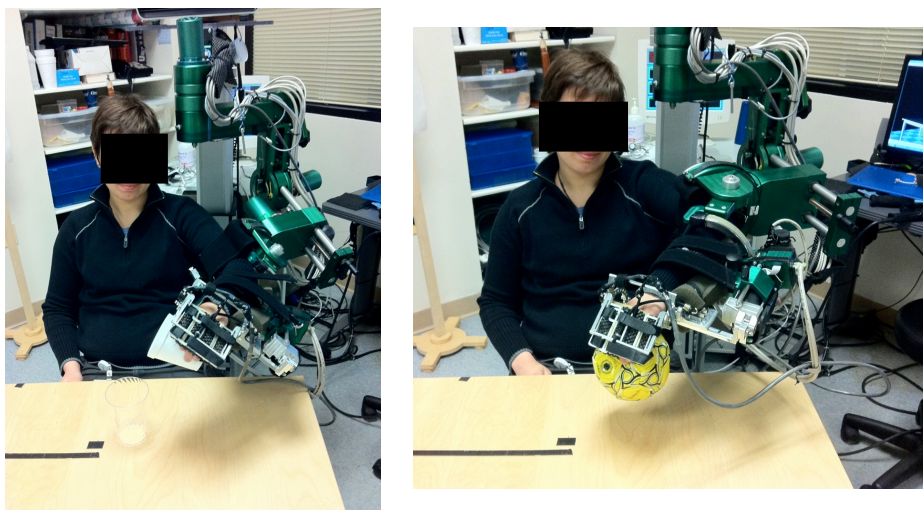
Figure 4.5 The image on the left shows an individual pouring the contents of a cup onto a table. If the subject does not modulate their grasp the cup will be crushed and will not allow the contexts to pour from it. The right image shows a subject moving objects between the sides of the table in the Sorting task.

3. ARMIN TRAINING RESULTS

The subjects showed progress in task ability across the training sessions as examined through the evaluations done at the beginning of each task training session. Figure 4.6 shows the average improvements made in percentage of the task completed without assistance in evaluation at the beginning of each task. Subjects consistently completed more of each task across training. For Ltraj 100 % task completion is when the subject moves their shoulder to 90 degrees and supinates their wrist to ten degrees beyond neutral position. For the shelf task, 100% complete is reaches when the subject successfully elevated their shoulder and extended their elbow to the top of the shelf. For the Pouring

and Sorting tasks the subject also needed to return to the start position to reach 100% task completion.
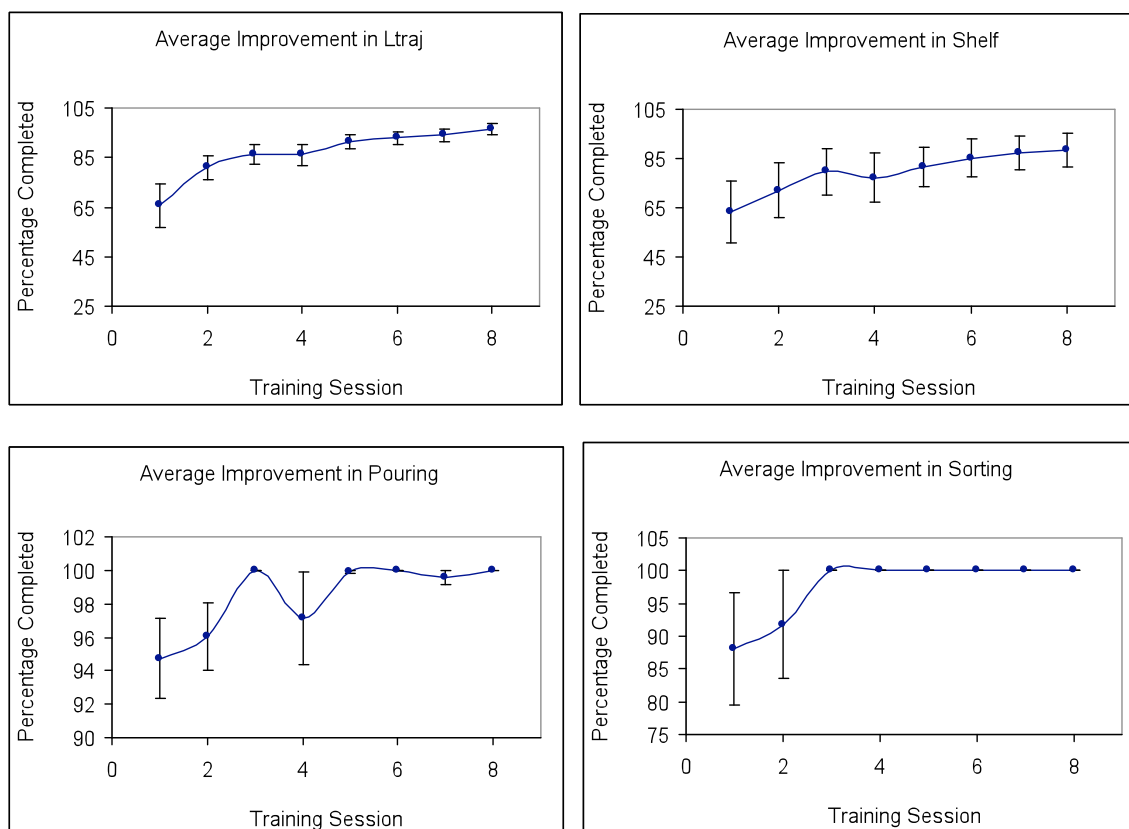
Figure 4.6 Average improvements in task completion in the robot without assistance over the eight training sessions. Standard error bars are presented.

Clinical Outcomes

The ARAT, Fugl Meyer, and Box and Blocks scores before and after robotic training are presented in Table 4.4. On average subjects improved by 1.55 points on the Fugl Meyer, 3.46 points on the ARAT, and 0.55 on the Box and Blocks. A paired t-test comparing the pre and post data showed significant change in the ARAT (p=0.01) from robotic training

but not in the Fugl Meyer (FM) (p=0.22) or Box and Blocks (BB) (p=0.57). All subjects had gains in at least one of the clinical measures after training.

Table 4.1 Clinical Measures Pre and Post Robotic Training

Subject	Before Training			After Training		
	FM	ARAT	BB	FM	ARAT	BB
1	22	21	0	25	19	0
2	13	14	0	17	17	0
3	26	9	0	22	18	2
4	23	19	2	25	20	3
5	34	29	11	33	36	9
6	21	26	14	22	23	14
7	17	16	1	15	21	1
8	18	13	6	25	19	5
9	31	30	4	29	35	13
10	15	9	0	15	13	0
11	34	44	38	43	47	35

4. CONCLUSIONS

The TIFT training paradigm with the ARMin III robot and the HandSOME device has shown promise as a rehabilitation tool. Eleven chronic stroke subjects completed the four week training with the robot and technician, no adverse events were reported and no subjects dropped out during training, showing that the system is well tolerated and subjects could understand the constraints of the TIFT mode. Subjects improved in robotic measures across training and each subject improved in at least one of the clinical measures. The ARAT improvement was statistically significant, showing that the ARMin training helped improve object manipulation. It is unfortunate that significant gains were not seen with the Fugl Meyer or Box and Blocks. This may be due to the relatively small

number of training sessions. The fact that gains were seen without daily interaction with a trained therapist is also encouraging for possible reduction of cost. Overall, the ARMin III and HandSOME system with the TIFT mode show potential for training functional tasks after stroke.

CHAPTER 5. CONCLUSIONS

As rehabilitation technologies progress, the focus needs to be on the improvement of a patient's function in daily life. The goals of functionally focused patient training are met with the HandSOME device with the ARMin III robot using the TIFT modality.

The HandSOME device allows for finger extension and grasp coordination assistance, both independently and with the ARMin III robot. The system is lightweight, thus limiting possible negative effects on the patient's shoulder or the robot's strength, and addresses the common issues of finger flexor hypertonia and the loss of joint coordination after stroke. The device leaves the palm free for real world object manipulation. Subjects were about to train grasp with objects of many different shapes, sizes and weights. The cross-sectional study showed that HandSOME device did improve subject's functional use of the hand when the device was on.

The TIFT mode focuses on retraining normal joint kinematics during functional task training. The cross-sectional study with neurologically normal subjects showed that even though the ability to learn a novel path may be the same for vision based, TD, and TIFT modes, TIFT subjects reduced their reliance on guiding forces during training, while TD subjects did not. In stroke subjects, we saw that the EPTT training allows for subjects to drag along the tunnel wall, having the robot assist their lagging joint. This meant that most of the subjects had less active movement and little to no active joint coordination during training compared to during training with the TIFT mode. In addition to not regaining normal joint coordination, it is expected that this compensation strategy would

limit therapeutic gains as was shown with the decreased activations in TD mode studies (Hidler 2009).

The HandSOME and TIFT mode were combined with the ARMin III robot and showed promise as a therapeutic intervention. Eleven chronic stroke subjects went through eight 1.5 hour sessions with the system. Subjects were able to understand the TIFT interface to complete the tasks, and work with real objects during training. On average the subjects showed steady improvement in the tasks between sessions and the subjects showed significant improvement in the ARAT score after the training protocol. All subjects improved in at least one of the clinical outcome measures. These results show that the combined training of grasp and joint control are possible and can lead to functional improvement after stroke.

APPENDIX 1. ROBOT GRAVITY COMPENSATION SOFTWARE

1. Check Angles Are Properly Calibrated

2. Set spring tightness to where the robot's resting shoulder angle is ~110˚

Process for recalibration of the spring

1. Dismounted robot, and spring, and measured the voltage to hold the shoulder at 90 degrees.

$$Ts+Tsp+Tm*sin(ThetaS)=0 \qquad\qquad (1)$$

Ts is the measured voltage converted into torque, Tsp is the spring's applied torque, Tm is the torque to hold the remaining weight, ThetaS is the angle of shoulder flexion

2. Reattached the spring and calculated the change in spring torque in increments of 2 inches.

$$Tsp(ThetaS)=-Ts-T_m sin(ThetaS)-T*sin(ThetaS) \qquad\qquad (2)$$

T* was an attached weight at a known distance to combat the positive torque of the spring at the shoulder. The weight was 10.82 lb at 30cm thus -14.43 Nm (negative since pulls down).

The following equation was used and converts the voltage measurements into torques.

$$T\_sp(i)=(-Torques(i)-T_m*sind(ThetaS(i)))/2*Kt(1)*Gear(1)-T\_star*sind(ThetaS(i)); \qquad (3)$$

The graph shows a plot with equation $y = -0.0068x^2 + 0.6747x + 19.307$ and $R^2 = 0.9793$, with "Angle in Degrees" on the x-axis.
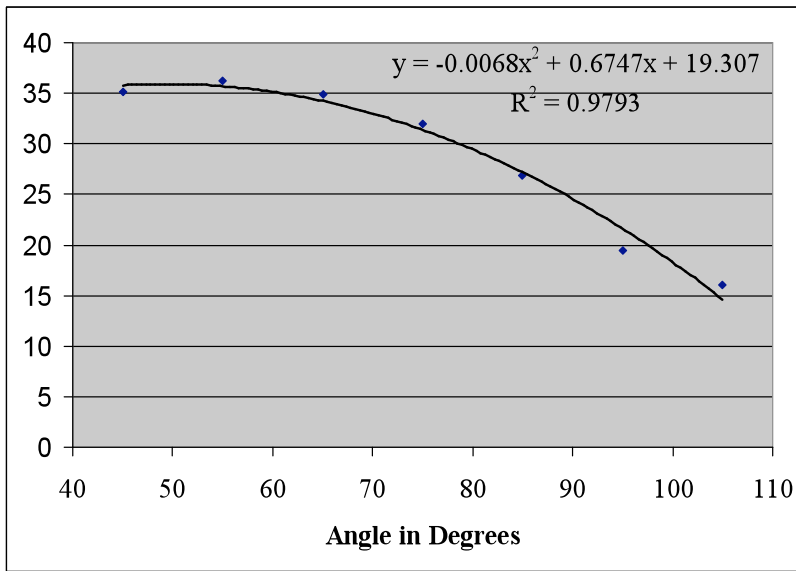
The best fit line was used to get the spring torque as a function of angle.

<u>Theory behind the gravity compensation torques</u>
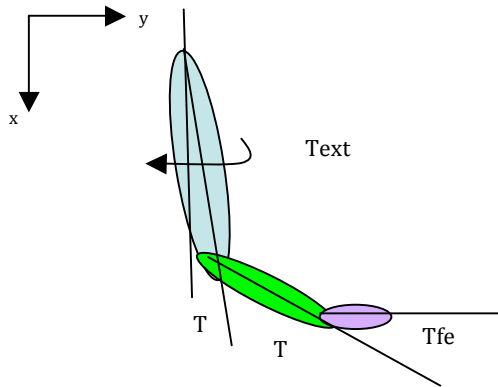
Shoulder Flex: +   Frame [1]

Elbow Flex: +   Frame [2]

Ext Rot: +   Frame [3]

Supination (Tsp): +   Frame [4]

99

The rotation matrices were found for each link.

$$
{}^0_1R = \begin{bmatrix} Cs & -Ss & 0 \\ Ss & Cs & 0 \\ 0 & 0 & 1 \end{bmatrix}
$$

From Zero Frame into the Shoulder Flexion Frame

$$
{}^1_2R = \begin{bmatrix} 1 & 0 & 0 \\ 0 & Cext & -Sext \\ 0 & Sext & Cext \end{bmatrix}
$$

$$
{}^0_2R = {}^0_1R * {}^1_2R
$$
External Rotation From the Zero Frame

$$
{}^2_3R = \begin{bmatrix} Ce & -Se & 0 \\ Se & Ce & 0 \\ 0 & 0 & 1 \end{bmatrix}
$$

$$
{}^0_3R = {}^0_2R * {}^2_3R
$$
Zero Frame into Elbow

$$
{}^3_4R = \begin{bmatrix} 1 & 0 & 0 \\ 0 & Csp & -Ssp \\ 0 & Ssp & Csp \end{bmatrix}
$$

$$
{}^0_4R = {}^0_3R * {}^3_4R
$$
[0] Frame into Supination/pronation Frame

$$
{}^4_5R = \begin{bmatrix} Cf\,e & Sf\,e & 0 \\ -Sf\,e & Cf\,e & 0 \\ 0 & 0 & 1 \end{bmatrix}
$$

$$
{}^0_5R = {}^0_4R * {}^4_5R \quad \textbf{[0] into Wrist flexion frame}
$$

The locations of the centers of mass are unknown so vectors of unknowns were used in the calculations.
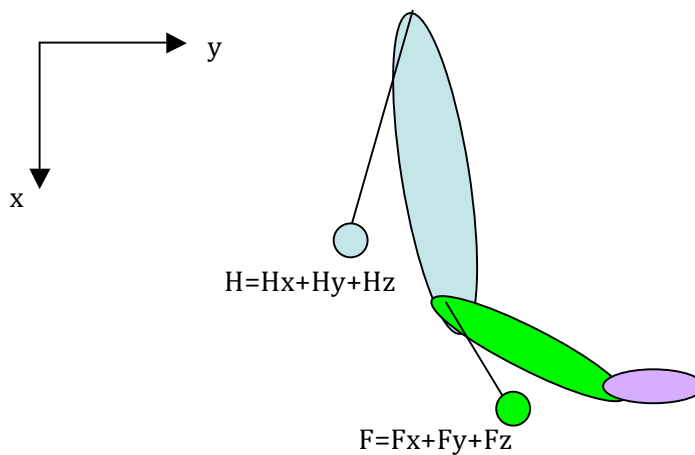
The wrist component was ignored for these calculations. Thus the vector H is the vector to the COM of the shoulder, and F is the vector to the COM of the forearm.

The Distances to the COM in the Zero Frame

$$
r_s = {}^0_2R * - {}^2\!\begin{bmatrix} H_x \\ H_y \\ H_z \end{bmatrix}
$$

$$r_e = {}_2^0R * - \begin{bmatrix} L_1 \\ 0 \\ 0 \end{bmatrix}^2 + {}_4^0R * - \begin{bmatrix} F_x \\ F_y \\ F_z \end{bmatrix}^4$$

The torque equations were obtained through the cross product of the vectors to the COM in the zero frame with the force of gravity

$$Moment_{Shoulder} = r_s \times \begin{bmatrix} m1g \\ 0 \\ 0 \end{bmatrix}^0 + r_e \times \begin{bmatrix} m2g \\ 0 \\ 0 \end{bmatrix}^0$$

The torque for shoulder flexion is the z component of the shoulder moment in the zero frame. This vector is described as follows.

$$z_s = {}_1^0R* \begin{bmatrix} 0 \\ 0 \\ 1 \end{bmatrix}^1$$

The torque for shoulder rotation is the x component of the shoulder moment in the zero frame. This vector is described as follows.

$$x_s = {}_2^0R* \begin{bmatrix} 1 \\ 0 \\ 0 \end{bmatrix}^2$$

The Torques are then calculated using the dot product of the two vectors

$$Torque_{SFlex} = Moment_{Shoulder} \cdot z_s$$

$$Torque_{EXT} = Moment_{Shoulder} \cdot x_s$$

The torque equations for the elbow were obtained through the cross product of the vectors to the COM in the zero frame with the force of gravity

$$Moment_{Elbow} = r_e \times {}^{0}\begin{bmatrix} m2g \\ 0 \\ 0 \end{bmatrix}$$

The torque for elbow flexion is the z component of the shoulder moment in the zero frame. This vector is described as follows.

$$z_e = {}_{3}^{0}R * {}^{3}\begin{bmatrix} 0 \\ 0 \\ 1 \end{bmatrix}$$

The torque for supination pronation is the x component of the shoulder moment in the zero frame. This vector is described as follows.

$$x_e = {}_{4}^{0}R * {}^{4}\begin{bmatrix} 1 \\ 0 \\ 0 \end{bmatrix}$$

The Torques are then calculated using the dot product of the two vectors

$$Torque_{EFlex} = Moment_{Elbow} \cdot z_e$$

$$Torque_{SUP/PRO} = Moment_{Elbow} \cdot x_e$$

Final Equations Used in the ARMin Code

ElbowFTorque=((-Cs*Sext^2*Se*m2gfx-Cs*Sext^2*m2gfy*Ce*Csp-Cext*m2gfx*Ss*Ce-m2gfx*Cs*Cext^2*Se+Cext*m2gfy*Csp*Ss*Se-m2gfy*Csp*Cs*Cext^2*Ce))*2/(Kt(4)*Gear(4));

ElbowSPTorque=-(-m2gfySP*Sext*Ce^2*Csp*Ss-m2gfySP*Cext*Ssp*Ss*Ce-m2gfySP*Cext^2*Ssp*Cs*Se+m2gfzSP*Sext*Ce^2*Ssp*Ss-m2gfzSP*Cext*Csp*Ss*Ce-m2gfzSP*Cext^2*Csp*Cs*Se-Sext*Se^2*m2gfySP*Csp*Ss-Sext^2*Se*m2gfySP*Cs*Ssp+Sext*Se^2*m2gfzSP*Ssp*Ss-Sext^2*Se*m2gfzSP*Cs*Csp)*2/(Kt(5)*Gear(5));

WristFTorque=0;

ShoulderRotTorque=0;

fcn=-(Ss*Ce+Cs*Cext*Se)*m2gfx-((-Ss*Se+Cs*Cext*Ce)*Csp-Cs*Sext*Ssp)*m2gfy;

ShoulderFTorque=sfac*((Ss*m1ghx_m2gl2-Cs*Cext*m1ghy+Cs*Sext*m1ghz+Ss*m1gdl_m2gdl+fcn-Tsp)*2/(Kt(1)*Gear(1))+0.1760*Ss);

ShoulderExtTorque=(((Sext*m1ghyEXT+Cext*m1ghzEXT)+(Sext*Se*m2gfx+(Sext*Ce*Csp+Cext*Ssp)*m2gfy))*Ss)*2/(Kt(3)*Gear(3));

Calculation of Center of Mass Locations

A. m2gfx: Set Te=0, Text=0, Ts=90

Elbow torque becomes (after conversion for elbow motor) **:**

T=-m2gfx

B. m2gfy Set Te=90, Text=0, Ts=90

Elbow torque becomes (after conversion for elbow motor) :

T=+m2gfy

C. m2gfz = = 0 Cancels out in calculations.

m2gfzSP Set Ts=90, Text=0, Te=0, Tsp=0

D. **m1ghx:** Ts=90; Text=0; Te=0; Tsp=0; Tfe=0;

Found as a set with the change in the length of the shoulder component.

At first dl was set to zero

Simplified the found torque equation: m1gdl_m2gdl=0; % (since dl=0) Reset Below

m1ghy=0; m1ghz=0;

T(1) is the torque at length equal to zero.

fcn=-(Ss*Ce+Cs*Cext*Se)*m2gfx-((-Ss*Se+Cs*Cext*Ce)*Csp-Cs*Sext*Ssp)*m2gfy;

m1ghx_m2gl2=(Cs*Cext*m1ghy-Cs*Sext*m1ghz-Ss*m1gdl_m2gdl-fcn+(T(1)))/Ss;

 Effect of change in the shoulder component length

T is the measured voltage at the shoulder in increments of 2 inches then converted into Nm and the torque of the spring subtracted

T=[0.65 1.65 2.75 4.025]/2*Kt(1)*Gear(1)+Tsp;

Tor=T-m1ghx_m2gl2-fcn1;

m1gdl_m2gdl=max(Tor)/max(L*2.54/100); %*dl;

E. **m1ghy:** ThetaS=45 (this is the minimum of the joint), ThetaExt=0; ThetaE=0; Tsp=0; Tfe=0;

Ty=(Tsmeasuredy)/2*Kt(1)*Gear(1)+Tsp

Fcn is the same as above but it has a different values due to the change of the angles the same is true of the spring torque value since the shoulder is now at 45

m1ghy=(Ss*m1ghx_m2gl2+Cs*Sext*m1ghz+fcn3-Ty)/(Cs*Cext); % Ss*m1gdl_m2gdl removed since dl=0

F. **m1ghz**

Same procedure as m1ghy except Text=90

Tz=(Tsmeasuredz)/2*Kt(1)*Gear(1)+Tsp;

m1ghz=(Tz-Ss*m1ghx_m2gl2+Cs*Cext*m1ghy-fcn2)/(Cs*Sext);

G. **m1ghyEXT**: ThetaS=90; ThetaExt=-90; ThetaE=0; Tsp=90; Tfe=0;

Torque= -m1ghyEXT

H. **m1ghzEXT**: ThetaS=90; ThetaExt=0; ThetaE=0; Tsp=0; Tfe=0;

Torque=m1ghzEXT

APPENDIX 2. ARM GRAVITY COMPENSATION SOFTWARE

The process for human arm gravity compensation is very similar to ARMin compensation. However, the centers of rotation are known and wrist supination/pronation has no effect.

The equations for center of mass and arm weight parameters were taken from "Research Methods in Biomechanics" by Gordon E. Robertson et al. 2004.

Table of Dempster Parameters

Segment	Endpoints (proximal to distal)	Segment mass/total person mass	Center of mass/ segment length
Upper arm	Glenohumeral joint to elbow center	0.0280	0.436
Forearm	Elbow to wrist center	0.022	0.682

The same coordinate frames from the ARMin gravity compensation calculations were used except the centers of mass are located on the local x axis at a known distance.
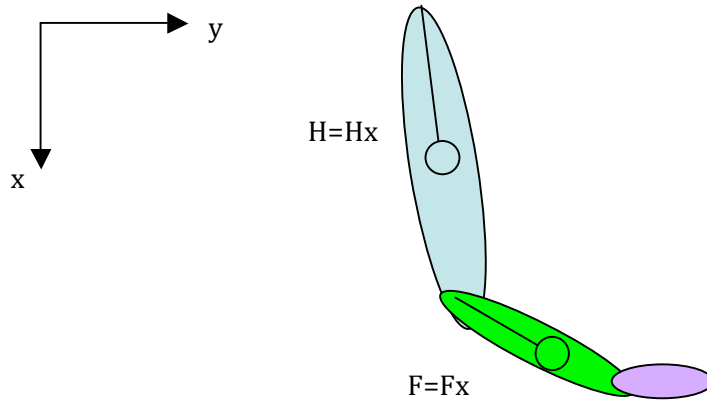
l_upper = The length of upper arm segment in meters, l_forearm = The length of the forearm segment in meters, m_total = The total mass of the subject in kilograms, m1g = upper arm mass force of gravity, m2g = forearm mass force of gravity, rs = vector to upper arm center of mass, re = vector to forearm center of mass

Location of Center of Mass

$$H = \begin{bmatrix} 0.436 * l\_upper \\ 0 \\ 0 \end{bmatrix} \text{ and } F = \begin{bmatrix} 0.682 * l\_forearm \\ 0 \\ 0 \end{bmatrix}$$

Segment masses component

$$m1g = 0.028 * 9.8 * m\_total \text{ and } m2g = 0.022 * 9.8 * m\_total$$

The rotation matrices remain the same as was calculated for the ARMin. From the information above we can calculate the distance to the joint centers in frame [0] as follows

$$r_s = {}_2^0R * - {}^2\begin{bmatrix} 0.436 * l\_upper \\ 0 \\ 0 \end{bmatrix}$$

$$r_e = {}_2^0R * - {}^2\begin{bmatrix} l\_upperarm \\ 0 \\ 0 \end{bmatrix} + {}_4^0R * - {}^4\begin{bmatrix} 0.682 * l\_forearm \\ 0 \\ 0 \end{bmatrix}$$

The torque equations were obtained through the cross product of the vectors to the COM in the zero frame with the force of gravity

$$Moment_{Shoulder} = r_s \times {}^0\begin{bmatrix} m1g \\ 0 \\ 0 \end{bmatrix} + r_e \times {}^0\begin{bmatrix} m2g \\ 0 \\ 0 \end{bmatrix}$$

The torque for shoulder flexion is the z component of the shoulder moment in the zero frame. This vector is described as follows.

$$z_s = {}_1^0R * {}^1\begin{bmatrix} 0 \\ 0 \\ 1 \end{bmatrix}$$

The torque for shoulder rotation is the x component of the shoulder moment in the zero frame. This vector is described as follows.

$$x_s = {}_2^0R * {}^2\begin{bmatrix} 1 \\ 0 \\ 0 \end{bmatrix}$$

The Torques are then calculated using the dot product of the two vectors

$$Torque_{SFlex} = Moment_{Shoulder} \cdot z_s$$

$$Torque_{EXT} = Moment_{Shoulder} \cdot x_s$$

The torque equations at the elbow were obtained through the cross product of the vectors to the COM in the zero frame with the force of gravity

$$Moment_{Elbow} = r_e \times {}^0\begin{bmatrix} m2g \\ 0 \\ 0 \end{bmatrix}$$

The torque for elbow flexion is the z component of the shoulder moment in the zero frame. This vector is described as follows.

$$z_e = {}^0_3R * {}^3\begin{bmatrix} 0 \\ 0 \\ 1 \end{bmatrix}$$

The torque for supination pronation is the x component of the shoulder moment in the zero frame, which is 0 in this case.

The Torques are then calculated using the dot product of the two vectors

$$Torque_{EFlex} = Moment_{Elbow} \cdot z_e$$

Final equations used in the ARMin code

ExtTorS = -183799/1250000*Sext*Se*l_forearm*m_total*Ss;

FlexTorS
=(52381/156250*Ss*l_upper+183799/1250000*(Ss*Ce*l_upper+Cs*Cext*Se*l_forearm
)) *m_total;

FlexTorE
=183799/1250000*m_total*l_forearm*(Sext^2*Se*Cs+Ss*Cext*Ce+Cext^2*Cs*Se);

These values are multiplied by a gain from 0 to 1 to change the amount of arm weight compensation, where 1 is 100% of the arm weight being compensated for.

REFERENCES

1. Aisen ML, Krebs HI, Hogan N, McDowell F, Volpe BT. The effect of robot-assisted therapy and rehabilitative train-ing on motor recovery following stroke. Arch Neurol. 1997; 54(4):443–46.

2. Balasubramanian S, Klein J, Burdet E. Robot-assisted rehabilitation of hand function. Curr Opin Neurol. 2010 Dec;23(6):661-70.

3. Banala SK, Kim SH, Agrawal SK, Scholz JP. Robot assisted gait training with active leg exoskeleton (ALEX). IEEE Trans Neural Syst Rehabil Eng. 2009;17(1):2–8.

4. Bohannon RW, Warren ME, Cogman KA. Motor variables correlated with the hand-to-mouth maneuver in stroke patients. Arch Phys Med Rehabil. 1991;72(9):682–84.

5. Bouzit M, Burdea G, Popescu G, Boian R., "The rutgers master II—new design force-feedback glove," *IEEE/ASME Trans. Mechatron.*, vol. 7, pp. 256-263, June 2002.

6. Bouzit, M., G. Burdea, G. Popescu, and R. Boian. "The Rutgers Master II-new design force-feedback glove." *IEEE/ASME Transactions on Mechatronics* 7, no. 2 (June 2002): 256-263.

7. Brokaw EB. Hand spring operated movement enhancer (HandSOME) device design for hand rehabilitation after stroke [MBE thesis]. Washington (DC): Catholic University of America; 2009.

8. Brokaw, EB, T Murray, and T Nef. "Retraining of interjoint arm coordination after stroke using robot-assisted time-independent functional training." *Journal of Rehabilitation Research and Development* (2011).

9. Brokaw, Elizabeth B, Iian Black, Rahsaan J Holley, and Peter S Lum. "Hand Spring Operated Movement Enhancer (HandSOME): a portable, passive hand exoskeleton for stroke rehabilitation." *IEEE transactions on neural systems and rehabilitation engineering: a publication of the IEEE Engineering in Medicine and Biology Society* 19, no. 4 (August 2011): 391-9.

10. Burger CG, Lum PS, Shor PC, Machiel HF. „Development of robots for rehabilitation therapy: the palo alto/standord experience" Journal of Rehabilitation Research and Development. Vol 37, no 6, pp 663-673, 2000.

11. Chengalur SN, Rodgers SH, Bernard TE. Kodak's Ergonomic Design for People at Work, 2nd Ed., Wiley, 2004 Table 1.5, pp 48 – 49.

12. Desrosiers J, Bravo G, Hebert R, Dutil E, Mercier L., "Validation of the Box and Block Test as a measure of dexterity of elderly people: reliability, validity, and norms studies," *Arch Phys Med Rehabil,* vol. 75, no. 7, pp.751-755, 1994.

13. Dewald JP, Beer RF. Abnormal joint torque patterns in the paretic upper limb of subjects with hemiparesis. Muscle Nerve. 2001;24(2):273–83. [PMID: 11180211] DOI:10.1002/1097-4598(200102)24:2<273::AID-MUS130>3.0.CO;2-Z 22.

14. Dipietro L, Krebs HI, Fasoli SE, Volpe BT, Stein J, Bever C, Hogan N. Changing motor synergies in chronic stroke. J Neurophysiol. 2007;98(2):757–68.

15. Donaldson, C., R. Tallis, Simon Miller, Alan Sunderland, Roger Lemon, and Valerie Pomeroy. "Effects of conventional physical therapy and functional strength training on upper limb motor recovery after stroke: a randomized phase II study." *Neurorehabilitation and neural repair* 23, no. 4 (May 2009): 389 97.

16. Duncan DW, Bode R.K., Min Lai S, Perera S., "Rasch analysis of a new stroke-specific outcome scale: the Stroke Impact Scale," *Arch Phys Med Rehabil*, vol, 84, pp. 950-63, Jul 2003

17. Ellis MD, Holubar BG, Acosta AM, Beer RF, Dewald JP. Modifiability of abnormal isometric elbow and shoulder joint torque coupling after stroke. Muscle Nerve. 2005;32(2): 170–78.

18. Farrell, John F, Henry B Hoffman, Janet L Snyder, Carol a Giuliani, and Richard W Bohannon. "Orthotic aided training of the paretic upper limb in chronic stroke: results of a phase 1 trial." *NeuroRehabilitation* 22, no. 2 (January 2007): 99-103.

19. Fischer, Heidi C, Kathy Stubblefield, Tiffany Kline, Xun Luo, Robert V Kenyon, and Derek G Kamper. "Hand rehabilitation following stroke: a pilot study of

assisted finger extension training in a virtual environment." *Topics in stroke rehabilitation* 14, no. 1 (2007): 1-12.

20. Fugl-Meyer A, Jääskö L, Leyman I, Olsson S, Steglind S, "The post-stroke hemiplegic patient. 1. a method for evaluation of physical performance," *Scand J Rehabil Med,* 1975. 7(1):13-31.

21. Gregson JM, Leathley M, Moore AP, Sharma AK, Smith TL, Watkins CL. "Reliability of the Tone Assessment Scale and the modified Ashworth scale as clinical tools for assessing poststroke spasticity," *Arch Phys Med Rehabil* 1999, 80(9):1013-1016.

22. Herder JL, Vrijlandt N, Antonides T, Cloosterman M, Mastenbroek PL, "Principle and design of a mobile arm support for people with muscular weakness," *J. Rehabil. Res. Develop.*, vol. 43, no. 5, pp. 591–604, Aug.–Sep. 2006

23. Hidler J, Nichols D, Pelliccio M, Brady K, Campbell DD, Kahn JH, Hornby TG. Multicenter randomized clinical trial evaluating the effectiveness of the Lokomat in subacute stroke. Neurorehabil Neural Repair. 2009;23(1):5–13.

24. Hornby TG, Campbell DD, Kahn JH, Demott T, Moore JL, Roth HR. Enhanced gait-related improvements after therapist- versus robotic-assisted locomotor training in subjects with chronic stroke: A randomized controlled study. Stroke. 2008;39(6):1786–92

25. Housman SJ, Scott KM, Reinkensmeyer DJ. A randomized controlled trial of gravity-supported, computer-enhanced arm exercise for individuals with severe hemiparesis. Neu-rorehabil Neural Repair. 2009;23(5):505–14.

26. Housman SJ, Scott KM, Reinkensmeyer DK. "A Randomized Controlled Trial of Gravity-Supported, Computer-Enhanced Arm Exercise for Individuals With Severe Hemiparesis." Neurorehabilitation and Neural Repair, February 23, 2009.

27. Kahn LE, Lum PS, Rymer WZ, Reinkensmeyer DJ. Robot-assisted movement training for the stroke-impaired arm: Does it matter what the robot does? J Rehabil Res Dev. 2006;43(5):619–30. Burger 2000

28. Kahn LE, Lum PS, Rymer WZ, Reinkensmeyer DJ. Robot-assisted movement training for the stroke-impaired arm: Does it matter what the robot does? J Rehabil Res Dev. 2006;43(5):619–30.

29. Kamper, D G, and W Z Rymer. "Quantitative features of the stretch response of extrinsic finger muscles in hemiparetic stroke." *Muscle & nerve* 23, no. 6 (June 2000): 954-61.

30. Kamper, DG, RL Harvey, S Suresh, and WZ. "Relative contributions of neural mechanisms versus muscle mechanics in promoting finger extension deficits following stroke." *Muscle &* 28, no. September (2003): 309-318.

31. Krakauer JW. Motor learning: Its relevance to stroke recov-ery and neurorehabilitation. Curr Opin Neurol. 2006;19(1): 84–90.

32. Lance, J. W. The control of muscle tone, reflexes, and movement: Robert Wartenberg Lecture. *Neurology* 30:1303 – 1313, 1980.

33. Lai SM, Studenski S, Duncan PW, Perera S. Persisting con-sequences of stroke measured by the Stroke Impact Scale. Stroke 2002;33(7):1840-44

34. Lambercy O, Dovat L, Gassert R, Burdet E, Teo CL, Milner T. "A haptic knob for rehabilitation of hand function," *IEEE Trans. Neural Syst.* Rehabil. Eng., vol. 15, pp. 356-366, 2007

35. Lang, Catherine E, and Marc H Schieber. "Reduced muscle selectivity during individuated finger movements in humans after damage to the motor cortex or corticospinal tract." *Journal of neurophysiology* 91, no. 4 (April 2004): 1722-33.

36. Liu J, Cramer SC, Reinkensmeyer DJ. Learning to perform a new movement with robotic assistance: Comparison of haptic guidance and visual demonstration. J Neuroeng Rehabil. 2006;3:20.

37. Lum PS, Burgar CG, Shor PC, Majmundar M, Van der Loos M. Robot-assisted movement training compared with conventional therapy techniques for the rehabilitation of upper-limb motor function after stroke. Arch Phys Med Rehabil. 2002;83(7):952–59

38. Lum PS, Burgar CG, Shor PC. Evidence for strength imbalances as a significant contributor to abnormal synergies in hemiparetic subjects. Muscle Nerve. 2003;27(2):211–21.

39. Lum PS, Mulroy S, Amdur RL, Requejo P, Prilutsky BI, Dromerick AW. Gains in upper extremity function after stroke via recovery or compensation: Potential differential effects on amount of real-world limb use. Top Stroke Rehabil. 2009;16(4):237–53.

40. Marchal-Crespo L, McHughen S, Cramer SC, Reinkens-meyer DJ. The effect of haptic guidance, aging, and initial skill level on motor learning of a steering task. Exp Brain Res. 2010;201(2):209–20.

41. Marteniuk RG, Leavitt JL, MacKenzie CL, Athenes S (1990) Functional relationships between grasp and transport components in a prehension task. Hum Mov Sci 9: 149–176

42. Masia L, Krebs HI, Cappa P, Hogan N, "Design and characterization of hand module for whole-arm rehabilitation following stroke," *IEEE/ASME Trans. Mechatron.*, vol. 12, pp. 399-407, August

43. Mastenbroek B, de Haan E, van Den Berg M, Herder JL, "Development of a Mobile Arm Support (Armon): Design Evolution and Preliminary User Experience," *IEEE 10th International Conference on Rehabilitation Robotics*, Noordwijk: 2007, pp. 1114-1120.

44. Nef T, Mihelj M, Riener R. ARMin: A robot for patient-cooperative arm therapy. Med Biol Eng Comput. 2007; 45(9):887–900.

45. Nichols-Larsen DS, Clark PC, Zeringue A, Greenspan A, Blanton S. Factors influencing stroke survivors' quality of life during subacute recovery. Stroke. 2005;36(7):1480–84.

46. Prange GB, Jannink MJ, Stienen AH, van der Kooij H, Ijzerman MJ, Hermens HJ. "Influence of gravity compensation on muscle activation patterns during different temporal phases of arm movements of stroke patients" Neurorehabil Neural Repair. 2009 Jun;23(5):478-85.

47. Raghavan, Preeti, Electra Petra, John W Krakauer, and Andrew M Gordon. "Patterns of impairment in digit independence after subcortical stroke." *Journal of neurophysiology* 95, no. 1 (January 2006): 369-78.

48. Rahman T, Sample W, Seliktar R, Scavina MT, Clark AL, Moran K, Alexander MA, Alfred I, "Design and testing of a functional arm orthosis in patients with neuromuscular disease," *IEEE Trans. Neural Syst. Rehabil. Eng.*, vol. 15, no. 2, pp. 244–251, Jun. 2007.

49. Rahman T, W. Sample, R Seliktar, M.T. Scavina, AL Clark, K Moran, MA Alexander, I Alfred. "Design and testing of a functional arm orthosis in patients with neuromuscular disease." *IEEE Transactions on Neural Systems and Rehabilitation Engineering*, June, 2007. 15(2):244-251.

50. Riener R, Nef T, Colombo G. Robot-aided neurorehabilita-tion of the upper extremities. Med Biol Eng Comput. 2005; 43(1):2–10.

51. Roby-Brami A, Feydy A, Combeaud M, Biryukova EV, Bussel B, Levin MF. Motor compensation and recovery for reaching in stroke patients. Acta Neurol Scand. 2003; 107(5):369–81.

52. Roger, V. L., a. S. Go, D. M. Lloyd-Jones, E. J. Benjamin, J. D. Berry, W. B. Borden, D. M. Bravata, et al. "Heart Disease and Stroke Statistics--2012 Update: A Report From the American Heart Association." *Circulation* (December 15, 2011): 12-230.

53. Rohrer B, Fasoli S, Krebs HI, Hughes R, Volpe B, Frontera WR, Stein J, Hogan N. Movement smoothness changes during stroke recovery. J Neurosci. 2002; 22(18):8297–304.

54. Sangani SG, Starsky AJ, McGuire JR, Schmit BD. Multi-joint reflexes of the stroke arm: Neural coupling of the elbow and shoulder. Muscle Nerve. 2007;36(5):694–703.

55. Stefan K, Kunesch E, Cohen LG, Benecke R, Classen J. Induction of plasticity in the human motor cortex by paired associative stimulation. Brain. 2000;123(3):572–84.

56. Stienen AHA, Hekman EEG, Van der Helm FCT, Prange, GB, Jannink MJA, Aalsma AMM, H. Van der Kooij. "Freebal: dedicated gravity compensation for upper extremities". Rehabilitation Robotic, 2007 ICORR. IEEE 10th International Conference: 804-808.

57. Stienen AHA, Hekman EEG, Van der Helm FCT, Prange, GB, Jannink MJA, Aalsma, A.M.M. Van der Kooij, H. "Dampace: dynamic force-coordination trainer for the upper extremities" Proceedings of the 2007 IEEE 10th International Conference on Rehabilitation Robotics, June 12-15, Noordwijk, The Netherlands.

58. Sukal TM, Ellis MD, Dewald JP. Shoulder abduction-induced reductions in reaching work area following hemi-paretic stroke: Neuroscientific implications. Exp Brain Res. 2007;183(2):215–23.

59. Taub E., Uswatte G., Elbert T, "New treatments in neurorehabilitation founded on basic research," *Nat Rev Neurosci*, vol. 3, no. 3, pp. 228-36, Mar 2002.

60. Timmermans AA, Seelen HA, Willmann RD, Kingma H,"Technology-assisted training of arm-hand skills in stroke: Concepts on reacquisition of motor control and therapist guidelines for rehabilitation technology design," *J. Neuroeng. Rehabil.*, vol. 6, pp. 1–1, 2009

61. Van Peppen, Rps, G Kwakkel, S Wood-Dauphinee, Hjm Hendriks, Phj Van der Wees, and J Dekker. "The impact of physical therapy on functional outcomes after stroke: what's the evidence?" *Clinical Rehabilitation* 18, no. 8 (December 1, 2004): 833-862.

62. Van Vliet PM, Sheridan MR. Coordination between reach-ing and grasping in patients with hemiparesis and healthy subjects. Arch Phys Med Rehabil. 2007;88(10):1325–31

63. Yozbatiran N, Der-Yeghiaian L, Cramer SC. "A standardized approach to performing the Action Research Arm Test," *Neurorehabil Neural Repair*. 2008;22:78-90.

64. Zackowsk KM, Dromerick AW, Sahrmann SA, Thach WT, Bastian AJ. How do strength, sensation, spasticity and joint individuation relate to the reaching deficits of people with chronic hemiparesis? Brain. 2004;127(Pt 5):1035–46.